UDOT's CALIBRATION OF AASHTO's NEW PRESTRESS LOSS DESIGN EQUATIONS

Prepared For:

Utah Department of Transportation
Research Division

Submitted By:

Utah State University
Department of Civil & Environmental
Engineering

Authored By:

Paul Barr
Marv Halling
Shane Boone
Raul Toca
Franklan Angomas

July 2009

DISCLAIMER:

The authors alone are responsible for the preparation and accuracy of the information, data, analysis, discussions, recommendations, and conclusions presented herein. The contents do not necessarily reflect the views, opinions, endorsements, or policies of the Utah Department of Transportation of the US Department of Transportation. The Utah Department of Transportation makes no representation or warranty of any kind, and assumes no liability therefore.

Technical Report Documentation Page

1. Project No. UT-09.10	2. Government Accession No.	3. Recipient's Catalog No.
4. Title and Subtitle UDOTs CALIBRATION OF AASHTO's NEW PRESTRESS LOSS DESIGN EQUATIONS		5. Report Date July, 2009
		6. Performing Organization Code
7. Author(s) Paul J. Barr, Marv Halling, Shane Boone, Raul Toca and Franklin Angomas		8. Performing Organization Report No. UTCM 09-10
9. Performing Organization Name and Address Utah State University Department of Civil and Environmental Engineering Logan, UT 84322-4110		10. Work Unit No. (TRAIS) 5H06051H
		11. Contract or Grant No. 079114
12. Sponsoring Agency Name and Address Utah Department of Transportation 4501 South 2700 West Salt Lake City, Utah 84114-8410		13. Type of Report and Period Covered Final Report 07/07 – 07/09
		14. Sponsoring Agency Code PIC No. UT06.802
15. Supplementary Notes Prepared in cooperation with the Utah Department of Transportation, U.S. Department of Transportation, and Federal Highway Administration		

16. Abstract

In the next edition of the AASHTO LRFD Bridge Design Specifications the procedure to calculate prestress losses will change dramatically. The new equations are empirically based on high performance concrete from four states (Nebraska, New Hampshire, Texas and Washington). The material testing resulted in modified equations to predict elastic shortening, shrinkage and creep. Because high performance concrete has traditionally resulted in smaller prestress losses these new equations also estimate lower losses in comparison to the existing equations. Many of the bridges built in Utah do not use specifically high performance concrete, but a self consolidating concrete that is different than the mixes that were used to develop the new AASHTO equations. Appropriate design parameters need to be established in order to apply them in the new AASHTO LRFD prestress loss calculations. This report summarizes the calibration of the AASHTO prestress loss equations for UDOT.

17. Key Word Prestress losses, bridge design, high strength concrete	18. Distribution Statement UDOT Research Division 4501 south 2700 West-box 148410 Salt Lake City, Utah 84114		
19. Security Classif. (of this report) Unclassified	20. Security Classif. (of this page) Unclassified	21. No. of Pages 66	22. Price n/a

ACKNOWLEDGEMENTS

EXECUTIVE SUMMARY

In the next edition of the AASHTO LRFD Bridge Design Specifications the procedure to calculate prestress losses will change dramatically. The new equations are empirically based on high performance concrete from four states (Nebraska, New Hampshire, Texas and Washington). The material testing resulted in modified equations to predict elastic shortening, shrinkage and creep. Because high performance concrete has traditionally resulted in smaller prestress losses these new equations also estimate lower losses in comparison to the existing equations. Many of the bridges built in Utah do not use specifically high performance concrete, but a self consolidating concrete that is different than the mixes that were used to develop the new AASHTO equations. Appropriate design parameters need to be established in order to apply them in the new AASHTO LRFD prestress loss calculations.

The main object of this research is to determine the appropriate design parameters that should be used in order to more accurately account for the prestress losses in precast, prestressed concrete bridges built within the state of Utah. This research was accomplished in two fold: 1-obtain design parameters elastic modulus(i.e., k_1 and k_2 for the elastic modulus) shrinkage and creep for typical Utah concrete girders mixes and 2- quantify the effects of deck casting and differential shrinkage on prestress gains to be used in the new procedures.

In order to accomplish these objectives, this report describes the measured behavior of six, high performance, self-consolidating concrete (HPSCC), prestressed bridge girders using embedded vibrating wire strain gages (VWSG). This instrumented bridge was part of the new Legacy Highway. State Street Bridge 669 of the Legacy Parkway in Farmington, Utah was designed by UDOT engineers as a precast, prestressed three-span bridge. The bridge was designed as simply supported for girder and deck self weight and three-span continuous for live load and superimposed dead weight. The first, second, and third spans are 132.2 feet, 108.5 feet, and 82.2 feet, respectively. The bridge had a width of 76.3 feet and a skew of approximately 25°.

Eleven AASHTO Type VI precast, prestressed girders spaced at 6.9 feet on center were used to support the 8 in. thick composite bridge deck for each span (Fig. 3.2(a)). Each girder contained 0.5 in. diameter low relaxation prestressing strands harped at 0.4 times the span length for each girder. The concrete strengths and number of prestressing strands for each girder were designed based on an HL-93 loading per AASHTO LRFD 2004 Bridge Design Specifications. Using these design criteria the first, second, and third spans were required to have 66, 39, and 26 strands in each girder, respectively. The specified compressive strength for all girders was 6.5 ksi and 7.5 ksi at release of the prestressing strands and 28 days, respectively. The 28 day design compressive strength specified for the composite deck concrete was 4 ksi. The measured strains for the VWSGs were used to determine prestress losses that were compared to calculated values obtained using the 2004 and 2007 AASHTO LRFD Specifications.

In addition to monitoring the in service bridge girders, measurements were also made on material specimens of the bridge girders. Additionally, representative concrete mixes from

Encon Precast was obtained in order to obtain a representative sample of all of UDOT prestressed girders.

The measured data from the bridge girders and from the material samples led to the following conclusions and recommendations:

1. Based on the findings from other researchers, the elastic modulus and creep losses are the most critical component to obtain in the design process.

2. Based on the elastic modulus results and the concrete compressive strengths and analysis were performed in order to determine the values for K_1 and K_2 to be used in the design of prestressed members in the state of Utah. The analysis resulted in a K_1 value of 0.896 and an upper bound for K_2 of 1.07 and a lower bound of 0.93. The lower value of K_1 is a result of the lower modulus of elasticity of the concrete relative to the proposed equation.

3. The average shrinkage strain that was measured from the material samples of typical UDOT concrete girder mixes was 430×10^{-6}. This is close to the recommended value of 480×10^{-6}. It is the recommendation of the researchers to use the recommended value as it is close to the measured value and conservative.

4. At 180 days, the concrete mix from Eagle precast had a creep coefficient of 1.6 whereas the creep coefficient for the Encon mix was nearly 2.1. The higher creep coefficient for the Eagle Precast mix is presumably due to the higher strength concrete. Because there is such a wide range, it is the recommendation of the researchers to use the recommended value of 1.9.

5. AASHTO LRFD 2007 Specifications predicted the total prestress loss within 3.7% and 7.9% for the 132 ft. and 82 ft. girders, respectively. In contrast, the predictions calculated using the AASHTO LRFD 2004 Specification were 76.4% and 125% overestimates of the total prestress losses measured for the 132 ft. and 82 ft. girders, respectively. Finally, the AASHTO LRFD 2004 Refined method predicted losses within 16.5% and 59.2% of the measured losses for the 132 ft. and 82 ft. girders, respectively. The AASHTO Lump sum method was within 6% of the measure long span girder, but was twice as large as the measured values for the short span girders. It is the recommendation of the researchers to use the new AASHTO method.

6. It was estimated that the stress loss due to differential shrinkage of the deck and girder concrete was relatively small (around 1 ksi) in compared with the other prestress losses. The new AASHTO method adequately predicted this loss and it is recommended to use this method.

TABLE OF CONTENTS

LIST OF FIGURES

LIST OF TABLES

CHAPTER 1 INTRODUCTION AND PREVIOUS RESEARCH

1.1 Problem Definition

In the next edition of the AASHTO LRFD Bridge Design Specifications the procedure to
calculate prestress losses will change dramatically. The new equations are empirically based on
high performance concrete from four states (Nebraska, New Hampshire, Texas and Washington).
The material testing resulted in modified equations to predict elastic shortening, shrinkage and
creep. Because high performance concrete has traditionally resulted in smaller prestress losses
these new equations also estimate lower losses in comparison to the existing equations. Many of
the bridges built in Utah do not use specifically high performance concrete, but a self
consolidating concrete that is different than the mixes that were used to develop the new
AASHTO equations. Appropriate design parameters need to be established in order to apply
them in the new AASHTO LRFD prestress loss calculations.

1.2 Objectives

The main object of this research is to determine the appropriate design parameters that
should be used in order to more accurately account for the prestress losses in precast, prestressed
concrete bridges built within the state of Utah. This research will be accomplished in two fold:
1- obtain design parameters elastic modulus(i.e., k_1 and k_2 for the elastic modulus) shrinkage and
creep for typical Utah concrete girders mixes and 2- quantify the effects of deck casting and
differential shrinkage on prestress gains to be used in the new procedures.

1.3 Project 18-07 Research

To date, the researchers associated with Project 18-07 have performed the only research in regards to quantifying the parameters for the newly proposed methods in the AASHTO LRFD Specifications. The researchers proposed a formula to calculate the modulus of elasticity of concrete that is based on two factors. The first factor is a k_1 value that represents the difference between the national average and a local average (if tests results with local materials are available). The second parameter, k_2, represents whether an upper-bound or a lower-bound value is desired in the calculations. The upper bound value would be a value that could be used for crack control purposes and a lower-bound value for prestress loss and deflection calculations. The proposed formula for elastic modulus calculations is:

$$E_c = 33,000 k_1 k_2 \left(0.140 + \frac{f'_c}{1000} \right)^{1.5} \sqrt{f'_c}$$

(1)

Where:

$k_1 = difference\ between\ national\ average\ and\ local\ average$

$k_2 = uppe\ and\ lower\ bound\ value$

In this equation, a correction factor of unity for the value of k_1 corresponds to an equal average of all predicted values and all measured values of modulus of elasticity. Concrete samples from five different regional areas were evaluated in order to come up with representative values for different regions. These obtained values are listed in Table 1.

2

Table 1-1 K-Values and Predicted to Measured Ratios of Modulus of Elasticity of Concrete (Tadros et al. 2002)

	Proposed k_1 and k_2			Ratio of Predicted to Measured	
	K_1	90-percentile k_2	10-percentile k_2	Proposed	AASHTO-LRFD
Nebraska (Medium Aggregate)	0.975	1.211	0.788	1.000	1.037
New Hampshire (Medium Aggregate)	0.911	1.123	0.878	1.000	1.122
Texas (Medium Aggregate)	1.282	1.150	0.850	1.000	0.751
Texas (Hard Aggregate)	1.359	1.079	0.921	1.000	0.785
Washington (Medium Aggregate)	1.154	1.182	0.817	1.000	0.889
All Data	1.000	1.224	0.777	1.020	1.037

In addition to providing guidelines in terms to calculating the elastic modulus of the concrete, the researchers also provided guidelines for calculating shrinkage values. The researchers state that in the absence of more accurate data, the ultimate shrinkage strain may be assumed to be 0.000480 in/in. A formula was also developed in order to determine the shrinkage values at any point in time. This equation was based on test data and a rectangular hyperbolic equation. The proposed equation to calculate the shrinkage effects is:

$$\varepsilon_{shrinkage} = 480 \times 10^{-6} k_{td} k_s k_{hs} k_f \qquad (2)$$

Where:

$$k_{td} = time\ development\ factor = \frac{t}{61 - 4.0 f'ci + t}$$

$$k_s = size\ factor = \frac{1064 - 94\,V/S}{735}$$

$$k_{hs} = humidity\ factor = 2.00 - 0.0143(H)$$

$$k_f = concrete\ strength\ factor = \frac{5}{1 + f'ci}$$

3

The equation to calculate the effect that creep has on prestressed concrete members was developed in the same manner as the shrinkage formulation. The ultimate creep coefficient for the standard conditions of relative humidity of 70%, volume-to-surface ratio of 3.5 in., initial concrete compressive strength of 4 ksi, loading age of 1 day for accelerated curing and 7 days for moist curing was found to be equal to 1.90. This value is comparable to the current AASHTO LRFD value. The creep effects can be calculated over time using the following proposed equation:

$$\psi(t, t_i) = 1.90 \gamma_{cr} k_1 \tag{3}$$

Where:

γ_{cr} = product of the applicable correction factors = $k_{td} k_{la} k_s k_{hc} k_f$

k_{td} = time development factor = $\dfrac{t}{61 - 4f'ci + t}$

k_{la} = loading factor = $t_i^{-0.118}$

k_{hc} = humidity factor for creep = $1.56 - 0.008H$

k_s = size factor = $\dfrac{1064 - 94 V/_S}{735}$

k_f = concrete strength factor = $\dfrac{5}{1 + f'ci}$

1.4 Bridge Instrumentation Studies

The measurement and prediction of prestress losses in HPC prestressed bridge girders is highly documented in literature. Kukay et al. (2007) presented a comparison of time dependent prestress losses in a two-span, prestressed concrete bridge. The four bridge girders studied in this investigation were made of HPSCC and were instrumented with vibrating wire strain gages with integral thermistors. The study compared values of prestress loss calculated from measured strain to predictive values found using the NCHRP 18-07 method. The study found that there was a relatively low percentage (11.5% of the jacking stress) of total measured prestress loss.

This smaller than expected loss was due to a significantly higher actual concrete strength than was required by design. Using the NCHRP design procedures, the study also found that when actual concrete strengths were used the predicted values of prestress losses corresponded closely with the measured values up through deck casting. After deck casting, the predicted values of total loss were found to be un-conservative when actual compressive strengths were used in the calculations.

Barr et al. (2007) instrumented and monitored five precast, prestress girder made with HPC. These girders were monitored for prestress losses for three years after the time of casting. The observed values of prestress losses were compared with values calculated using the AASHTO LRFD specifications (2004) and the methods based on the results of NCHRP 18-07 (Tadros et al. 2003). The study found that by using a calibrated modulus of elasticity, total losses calculated using the NCHRP method were within 10% of the measured total losses. However, this calibrated modulus resulted in the AASHTO calculated values being 30% higher than the total measured losses. The study found that, on average, the observed elastic shortening losses were found to be 21% higher than those calculated using AASHTO and 11% lower than those calculated using the NCHRP method. The difference between the measured and predicted losses was reduced to within 3% difference when the calibrated modulus was used.

Kowalsky et al. (2001) instrumented and measured prestress losses in several HPC bridge girders in North Carolina. The researchers found shrinkage losses were a small component of the overall prestress losses and that the elastic shortening and creep losses were the major contributors. These larger than expected losses from elastic shortening and creep were attributed to an actual modulus of elasticity that was lower than predicted. The total prestress losses ranged from 12.9% to 19.1% of the initial jacking stress.

Yang and Meyers (2005) instrumented four HPC prestressed bridge girders in Missouri with a total of 16 internal thermocouples, 64 VWSGs, and 14 internal bonded electrical resistance strain gages (ERSG). The researchers incorporated eight commonly used loss estimate models for calculating total prestress losses, including the AASHTO, Prestressed Concrete Institute (PCI), and NCHRP methods. They reported total measured average losses of 20.7% of the initial jacking stress with elastic shortening accounting for the largest portion of the total loss. Also, they concluded that for prestress precast HPC girders, the PCI handbook

method, the method recommended by Gross (1999), and the NCHRP method to be optimal for prestress losses estimation in the design.

Ahlborn et al. (1995) tested two full-size composite I-girders fabricated with HPC. Two different mix designs were used for these girders, which had a span length of 133 feet. Prestress losses predicted by incorporating measured material properties into the PCI general time step approach were 5 to 10 percent larger than measured in the instrumented girders.

Roller et al. (1995) fabricated and tested four prestressed high strength concrete bulb-tee girders. They found that the AASHTO 1989 LRFD Specifications provisions for calculating creep and shrinkage prestress losses may be overly conservative for high strength concrete. In their study, measured prestress losses were significantly less than the total long-term prestress losses predicted using the provisions in the AASHTO LRFD 1989 Specifications. They also found that measured creep and shrinkage deformations of cylinders representing the concrete in the instrumented girders were consistent with the finding regarding the measured prestress loss. Their study concluded that high strength bridge girders could be expected to perform adequately over the long-term when designed and fabricated in accordance with the 1989 AASHTO LRFD 1989 Specifications. However, the measured prestress losses in one of the girders instrumented was 50% less than the expected value indicating that the AASHTO LRFD 1989 Specifications were grossly conservative.

Additional literature regarding prestress losses in prestressed HPC bridge girders can be found in Cole (2000), Tadros et al. (2002), Stallings et al.(2003), and Gilbertson et al.(2004).

CHAPTER 2 DATA COLLECTION

In this chapter, the material test results are presented. Concrete samples were taken from Encon Precast and Eagle Precast in order to obtain design values to use in the AASHTO LRFD 2007 prestress equations. The concrete compressive strength, modulus of elasticity, shrinkage and creep were evaluated based on the concrete specimens that were taken. The results are discussed below.

2.1 Concrete Compressive Strength

Strength is defined as the ability to resist stress without failure. In compression the test specimen is considered to have failed even when no signs of external fracture are visible; however, the internal cracking has reached such an advanced state that the specimen is unable to carry a higher load.

The strength of concrete is the property most valued by designers and quality control engineers, and it is the property generally specified. This is because, compared to most other properties, testing of strength is relatively easy. Furthermore, many properties of concrete, such as elastic modulus, permeability, and resistance to weathering agents including aggressive waters, are believed to be a function of strength and may therefore be deduced from the strength data. Although in practice most concrete is subjected simultaneously to a combination of compressive, shearing, and tensile stresses in two or more directions, the uniaxial compression tests are the easiest to perform in laboratory, and the 28-day compressive strength of concrete determined by a standard uniaxial compression test is accepted universally as a general index of the concrete strength.

Although the actual response of concrete to applied stress is a result of complex interactions between various factors, to facilitate a clear understanding of these factors, they can be separately divided into three categories: (1) characteristics and proportions of materials, (2) curing conditions, and (3) testing parameters.

7

The compressive strength of concrete was measured in the laboratory by a uniaxial compression test (ASTM C 469) in which the load is progressively increased to fail the specimen within 2 to 3 min. It is evident that the actual loads (such as impact loads) and the loads under laboratory testing conditions vary. Therefore, it is important to have in mind that the loading condition has an important influence of the concrete strength.

For this project, 4" x 8" cylinders were cast in order to determine the concrete compressive strength. Each cylinder was submitted to the proper vibration, and finally placed in the fog room where it was allowed to cure. They were subsequently tested according to the ASTM C 31 and ASTM C 39, at each of the following days, from the day they were cast: 1, 3, 7, 14, 28, and 56 days.

Figure 2-1 Vibration of Concrete Specimens

Two cylinders were tested on each of the testing days, from which an average compressive strength was determined. The compressive strength was calculated using Equation 4.1, the compression machine is shown in Figure 4.2 and the results through the first 58 days are shown in Figure 4.3.

$$f = \frac{P}{A}$$

(Equation 4.1)

Where:

f = the compressive stress at any desired test day, and (f'c) being specifically the
    28 day compressive strength of tested specimens. (Psi)

P = failure load of the concrete specimen (lbs.)

A = the cross sectional area of the concrete specimen (in^2)

Figure 2-2 Compressive Strength Test
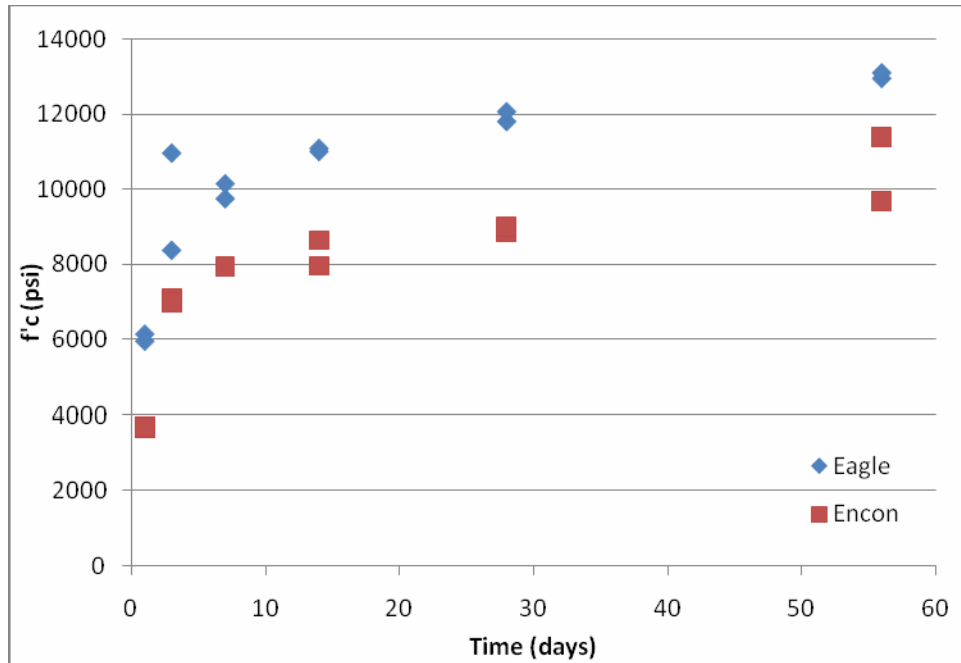
Figure 2-3 Concrete Compressive Strength versus Time

2.2 Modulus of Elasticity

Initially, when strain is proportional to the applied stress and is reversible on unloading the specimen, it is called the elastic strain. The modulus of elasticity is defined as the ratio between the stress and the reversible strain. The significance of the elastic limit lies in the fact that it represents the maximum allowable stress before the material undergoes permanent deformation. Therefore, the elastic modulus of the material influences the rigidity of a design.

For concrete, there is a direct relation between strength and elastic modulus, since both are affected by the porosity of the constituent phases, although not to the same degree. Several factors affect the modulus of elasticity of concrete. Among these are: aggregate, cement paste matrix, transition zone, and testing parameters.

The aggregate characteristic that most affects the elastic modulus of concrete is porosity. Dense aggregates have a high elastic modulus and the more of these aggregates in the concrete,

10

the higher the elastic modulus of the mix. Aggregate size, shape, surface texture, grading, and mineralogical composition also have an effect on the modulus of elasticity, since they can influence micro cracking, thus affecting the shape of the stress-strain curve.

The elastic modulus of the cement paste is determined by its porosity, which is in turn controlled by the water-cement ratio, air content, mineral admixtures, and degree of cement hydration.

The elastic modulus tests were performed at: 1, 3, 7, 14, 28, and 56 days after the time concrete samples. On each of the test days two specimens were tested. The compressive strength of the concrete was obtained on each testing day by using 4" x 8" cylinders, as previously described. The elastic modulus specimens (6" x 12") were then loaded to 40% of that compressive strength. By determining the slope of the resulting stress-strain curve, we were able to determine the modulus of elasticity of our concrete. Once the values of modulus of elasticity for each testing day were obtained a graph of modulus of elasticity vs. time was created. The test setup for the modulus of elasticity test is shown in Figure 4.4 and the test results are shown in Figure 4.5.

Figure 2-4 Modulus of Elasticity Test
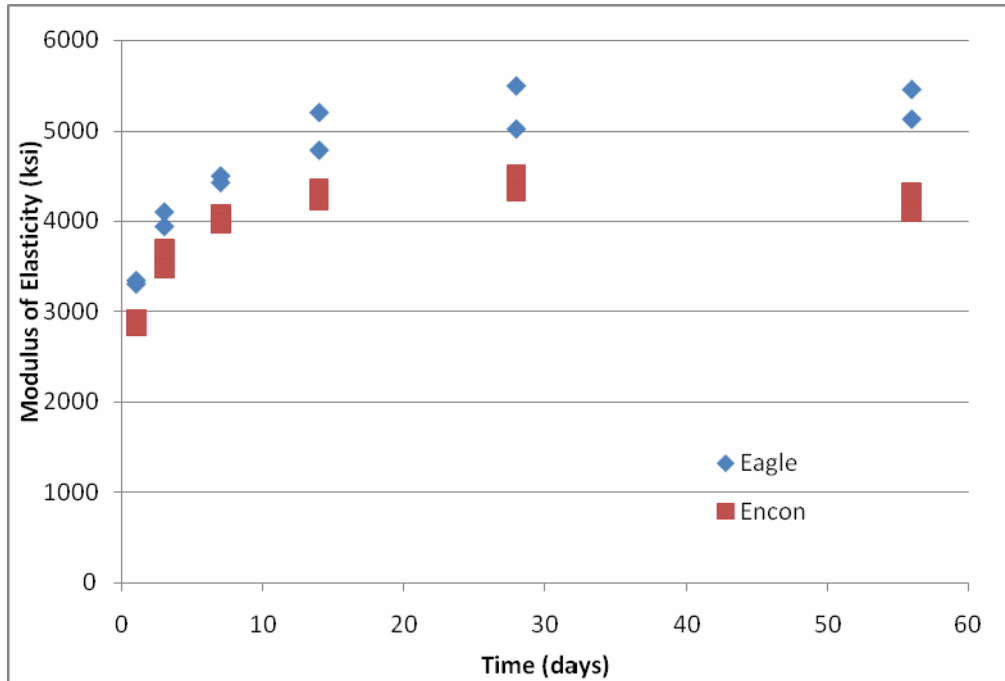
Figure 2-5 Modulus of Elasticity versus Time

Based on the elastic modulus results and the concrete compressive strengths and analysis were performed in order to determine the values for K_1 and K_2 to be used in the design of prestressed members in the state of Utah.   The analysis resulted in a K_1 value of 0.896 and an upper bound for K_2 of 1.07 and a lower bound of 0.93. The lower value of K_1 is a result of the lower modulus of elasticity of the concrete relative to the proposed equation.

2.3 Shrinkage

Shrinkage is the decrease (or swelling) of concrete when exposed to ambient humidity due to the removal of absorbed water (by evaporation) from the hydrated cement paste. Restraint to this shrinkage, provided by the reinforcement, or another part of the structure, causes tensile stresses to develop in the hardened concrete.

The ASTM C 157/C 157M testing procedures were used when testing the bridge deck concrete for shrinkage. The specimens were concrete prisms 3"x 3" x 16" in dimension. During

13

casting, metal studs were placed in the ends of each specimen to assist in monitoring the change in length of each specimen. The specimens were placed and kept completely submerged in water for a period of 14 days, prior to testing.

Shrinkage readings were taken in the comparator (Figure 2.6) at 3, 7, 14, 28, and 56 days. In total, changes in length of the two concrete specimens were monitored for 56 days.

Length change was calculated for each specimen at any age after the initial reading using Equation 2.2 and the results are shown in Figure 2.7.

$$\varepsilon = \frac{CRD - initial\ CRD}{G}$$ **(Equation 2.2)**

Where:

ε = Change in length of specimen at any age

CRD = Difference between the comparator reading of the specimen and the initial reading at any age.

G = Gage length (16 in.)

Figure 2-6 Shrinkage Test
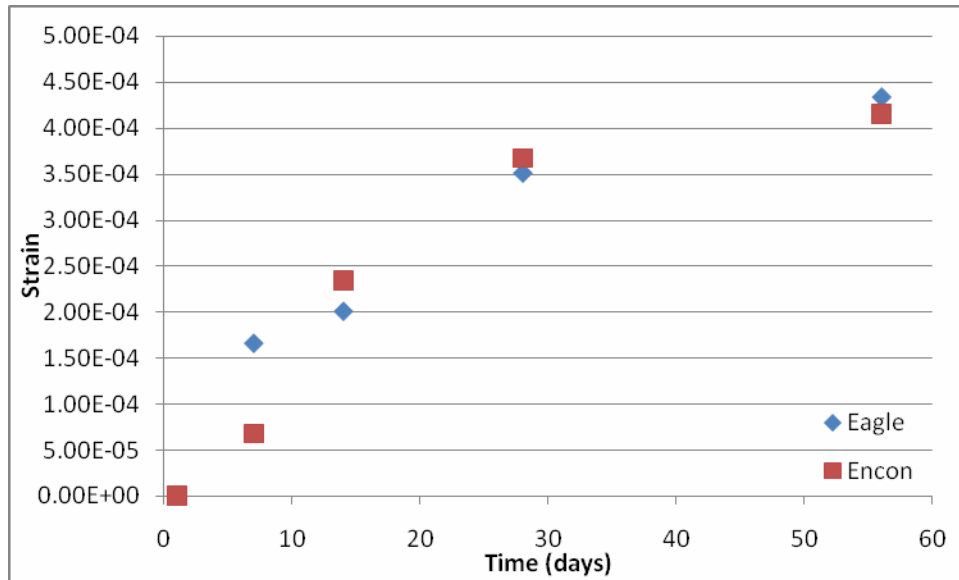
Figure 2-7 Shrinkage Strain versus Time

2.4 Creep

In prestressed concrete members, an important consequence of creep is that it leads to a substantial loss in prestress. To measure and quantify this effect, eight creep rigs were fabricated to apply a constant load to the specimens taken from the girder concrete. They were constructed in accordance with the creep test specifications of ASTM and are shown in Figure 2.8. The principle of the design is to apply a constant load to a stack of cylinders compressed between two steel plates by applying pressure with a pump beneath the lower plate and then locking in the load.

Five sets of two concentrically placed coil springs, supplied by Henry Miller Spring and Manufacturing Company of Pittsburgh, PA, were added to each creep rig to maintain the load nearly constant as the specimens shortened. The springs had a maximum compression of two inches, and an approximate stiffness of 2.35 kN/mm (13.4 k/in) for the spring with 203 mm (8 inch) outside-diameter (O.D.) and 1.14 kN/mm (6.5 k/in) for the 117 mm (4-$^5/_8$ in.) O.D. spring. Thus, the total stiffness of the five sets of springs was 17.5 kN/mm (100 k/in).

16
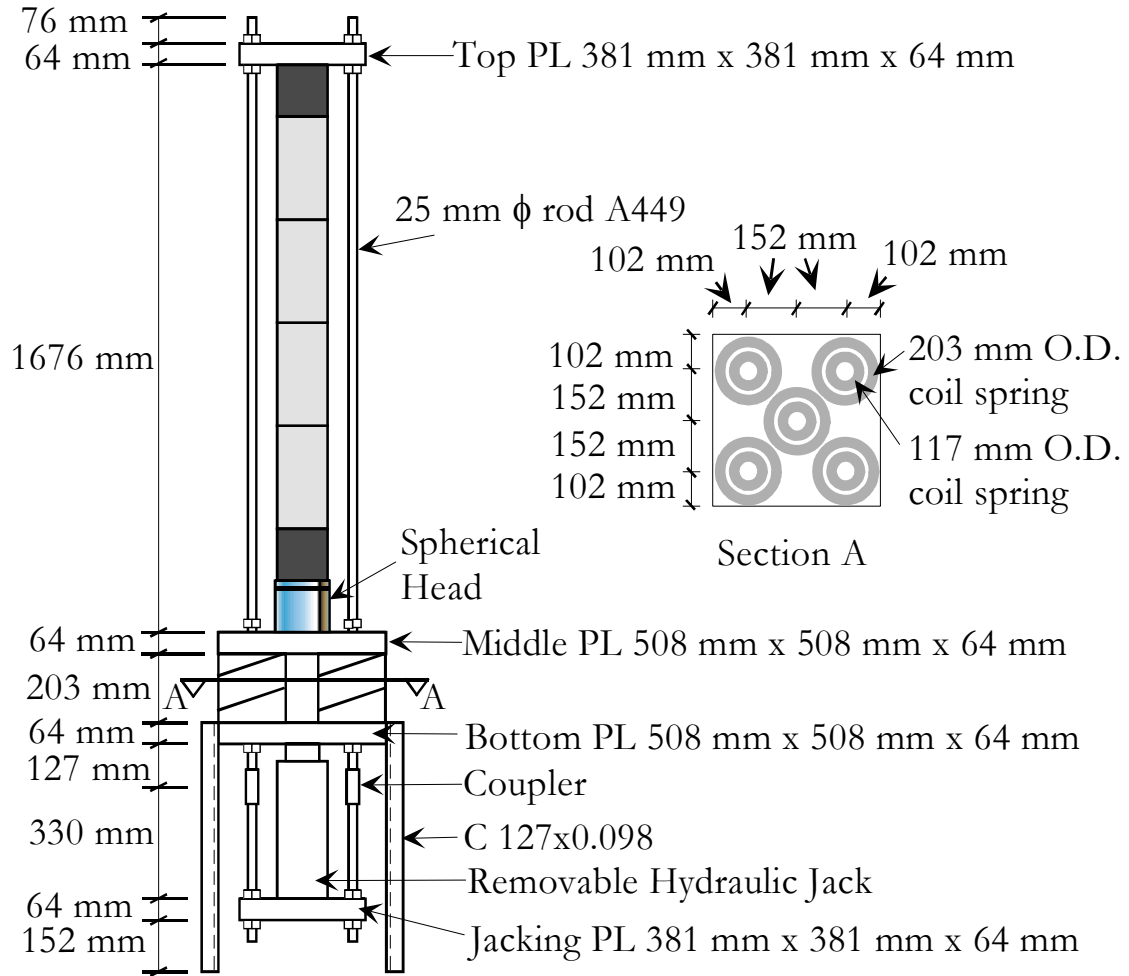
Figure 2-8 Creep Rig Design

To accommodate planned creep tests , 152 mm x 304 mm (6 in. x 12 in.) cylinders were cast. All cylinders were cast in oiled plastic molds. At least two sets of gage studs were attached on the sides of all the cylinders. Four sets were used on the specimens in order to preserve data even if a stud became detached from the cylinder. All sets of gage studs were attached in pairs across diameters with a 254-mm (10-inch) longitudinal separation. The two arrangements are shown in Figure 2.9.
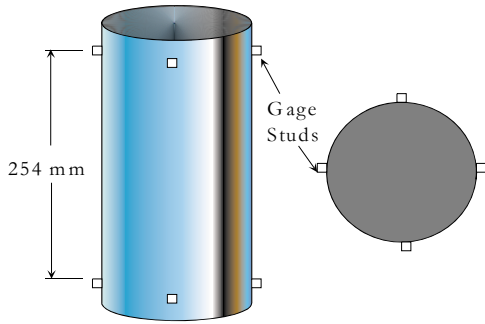
Figure 2-9 Gage Stud Locations

Figure 2-10 shows the creep coefficient calculated for the Eagle Precast and Encon Precast concrete mix designs. At 180 days, the concrete mix from Eagle precast had a creep coefficient of 1.6 whereas the creep coefficient for the Encon mix was nearly 2.1. The higher creep coefficient for the Eagle Precast mix is presumably due to the higher strength concrete.
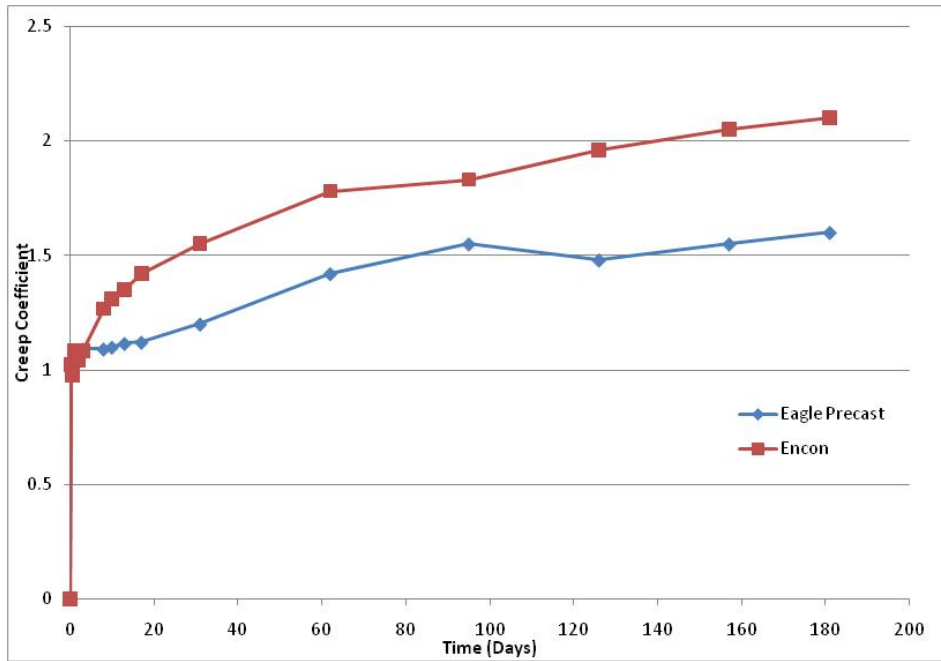
Figure 2-10 Creep Coefficient

CHAPTER 3 DATA EVALUATION/ANALYSIS

In this chapter, a comparison is made between the measured prestress losses and the calculated losses according to the AASHTO Standard, AASHTO LRFD and NCHRP 18-07 method. To accomplish this, girders from the Legacy Parkway Bridge (Bridge 669) were instrumented with vibrating-wire strain gages during fabrication. These gages monitored the change in strains and temperatures for nearly one year since the time of casting. These changes in strains were used to calculate the prestress losses for each of the instrumented girders. The background and results are presented in this chapter.

3.1 Legacy Parkway Bridge 669

State Street Bridge 669 of the Legacy Parkway in Farmington, Utah was designed by UDOT engineers as a precast, prestressed three-span bridge. The bridge was designed as simply supported for girder and deck self weight and three-span continuous for live load and superimposed dead weight. The first, second, and third spans are 132.2 ft., 108.5 ft., and 82.2 ft., respectively. The bridge had a width of 76.3 ft. and a skew of approximately 25°. Fig. 3.1 presents a typical elevation and cross sectional view of Bridge 669.

Eleven AASHTO Type VI precast, prestressed girders spaced at 6.9 ft. on center were used to support the 8 in. thick composite bridge deck for each span (Fig. 3.2(a)). Each girder contained 0.5 in. diameter low relaxation prestressing strands harped at 0.4 times the span length for each girder. The concrete strengths and number of prestressing strands for each girder were designed based on an HL-93 loading per AASHTO LRFD 2004 Bridge Design Specifications. Using these design criteria the first, second, and third spans were required to have 66, 39, and 26 strands in each girder, respectively (Fig. 3.2(b)). The specified compressive strength for all girders was 6.5 ksi and 7.5 ksi at release of the prestressing strands and 28 days, respectively. The 28 day design compressive strength specified for the composite deck concrete was 4 ksi.

The girders were placed in steel formwork and set to cure for 1 day before the formwork was removed and the prestress was transferred. There was no external heat or steam applied to the girders during curing. However, due to the low ambient temperatures, steam was released as the formwork was removed (Fig. 3.3).

Although the specified strengths of the girder concrete were relatively low, the fabricator elected to use a HPSCC mix design in part to reduce labor costs. As a result, the average compressive strengths at release and at 28 days were 8.4 ksi and 12.8 ksi, respectively. The average 28 day compressive strength of the composite deck concrete was 5.8 ksi. The composite deck was cast between approximately 2 and 5 months after the fabrication of the third and first spans, respectively.
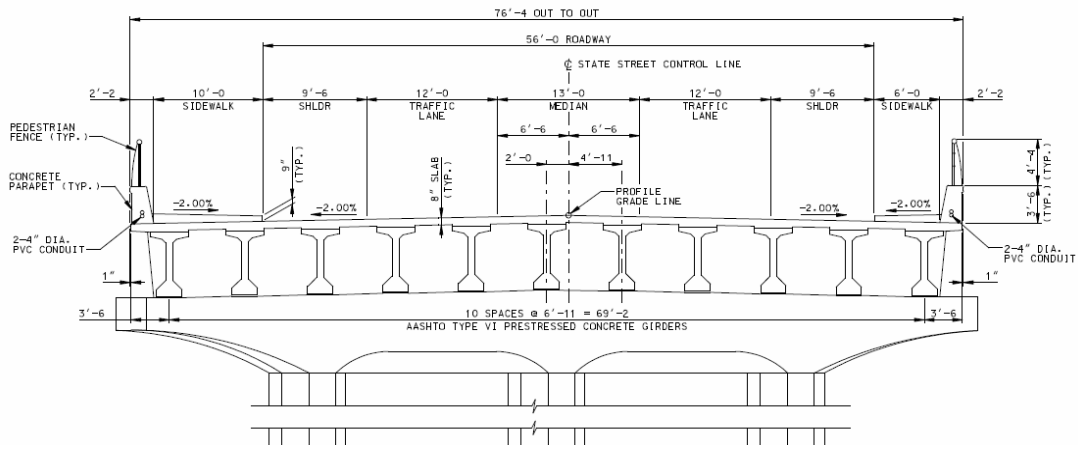
(a) Elevation view
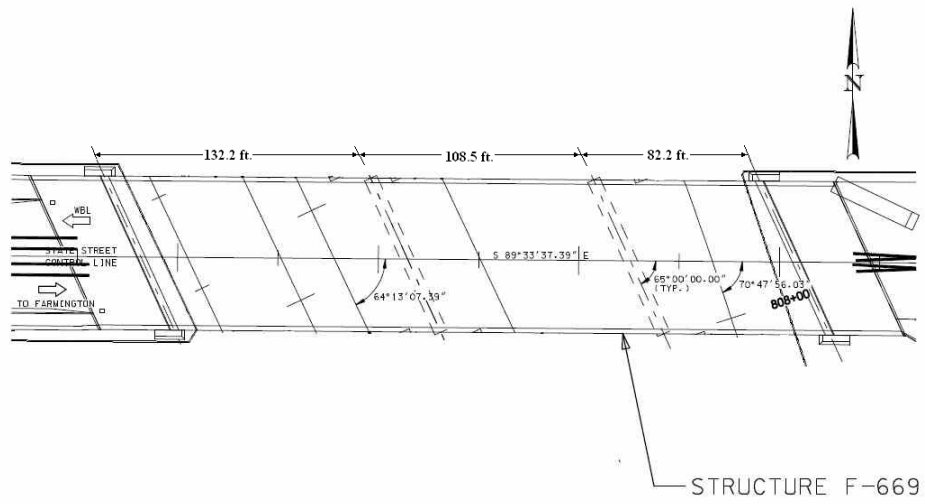
(b) Plan view

Figure 3-1 Bridge 669

(a) Typical AASHTO type VI girder

21
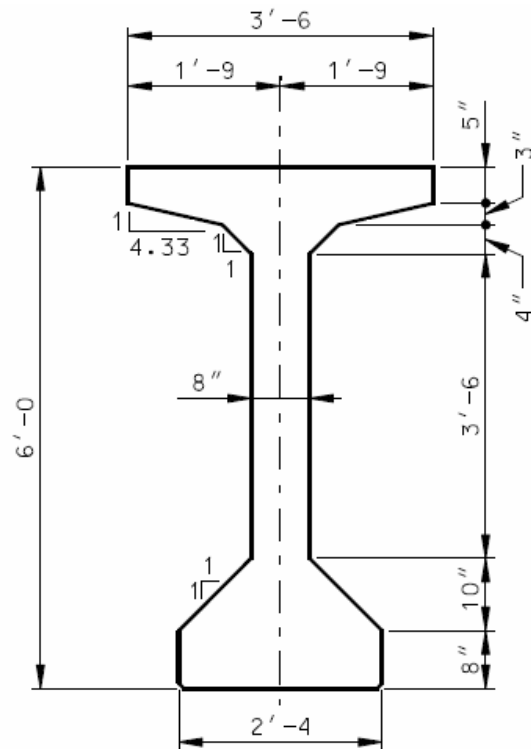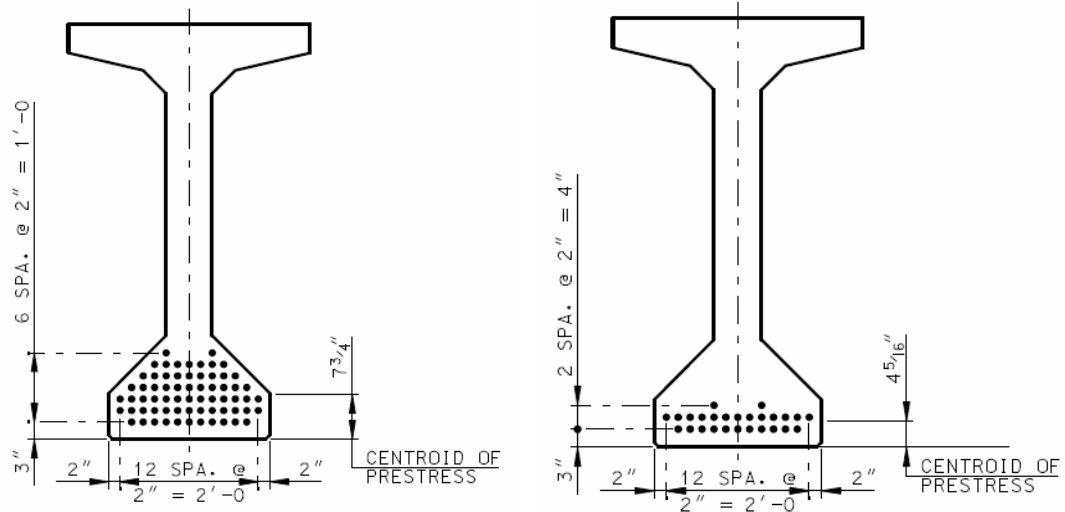
(b) Design of prestressing strands for first and third spans, respectively

(c) Girders in place before placement of composite concrete deck

Figure 3-2 Bridge 669 Girders

Figure 3-3 Girders were cured in steel forms with no external steam

3.2 Instrumentation and Monitoring Program

A total of 24 vibrating wire strain gages (VWSG) with integral thermistors were installed at midspan in the first and third spans of Bridge 669. Three girders from each span were instrumented with two VWSGs at the centroid of the prestressing strands and two VWSGs in the web of the girder. The centroid of the prestressing strands was 7.75 in. and 4.31 in. from the bottom of the girder for the 132 ft. and 82 ft. spans, respectively. The two VWSGs embedded in the web of the girder were installed at 29 in. and 59 in., respectively from the bottom of the girder (Fig. 3.4). These gages were embedded to obtain strain and temperature readings over the height of the section throughout time (Fig. 3.5). The gages measured variations in strain and temperature for approximately 10 months and 7 months for the first and third spans, respectively,

beginning at the time of casting. During distressing the gages were monitored every minute. During curing and placement the reading interval increased to fifteen minutes.

The large increase in strain at day 0 is due to elastic shortening and is caused by the transfer of prestress to the concrete girder when the prestressing strands are cut. The change in strain displayed at days 156 and 73 for the 132 ft. and 82 girders, respectively, is due to the deck placement. Strain gages in the top of the web experience an increase in strain during deck casting due to their position relative to the centroid of the composite section. Strain gages in the bottom of the web are closer to this centroid and thus see a smaller variation. The strain gages located at the strand centroid experience an increase in strain due to the deck placement. The gap in the data for both spans between transfer of prestress and deck casting was during transportation of the girders to the bridge site. At this time, the instrumentation was disconnected and no readings were recorded. The small change in strain shown directly after deck placement is due to the addition of super imposed dead load due to sidewalks and traffic barriers. The larger amount of prestress force and subsequent losses in the 132 ft. girder cause the strains measured and presented in Fig. 3.5(a) larger than those for the 82 ft. girder (Fig. 3.5(b)).

Figs. 3.6 – 3.7 presents the changes in temperature as a function of time for both the 132 ft. and 82 ft. spans, respectively. Each figure presents both the long term temperature readings (a) and temperature readings made during the first days of curing (b). During the first few days of curing the highest temperatures are achieved for both spans. As time progresses, the temperatures decrease as the initial curing temperature due to the hydration of the cement cease and ambient temperatures begin to control the temperature of the girder. The high temperatures due to the heat of hydration can be seen in Figs. 3.6(b) and 3.7(b). Temperatures during this phase of curing reach nearly 160° for both spans. It can also be noticed from these figures that the temperatures reached are higher in the web than in the flange. This is contrary to what might be expected. There is more concrete volume in the flange and the hydration should be more complete in this area of the girder than in the web.
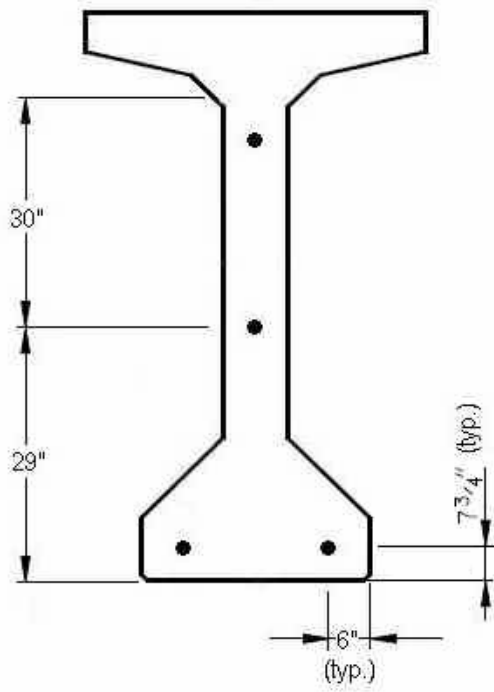
(a) 132 ft. girder
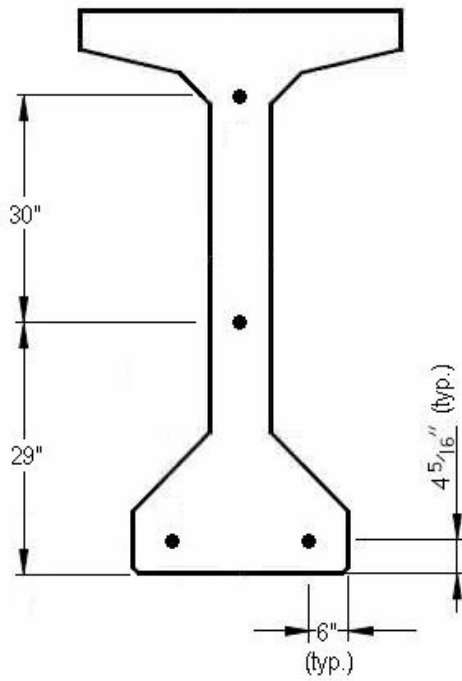
(b) 82 ft. girder

Figure 3-4 Location of Embedded VWSGs

25

(a) 132 ft. girder
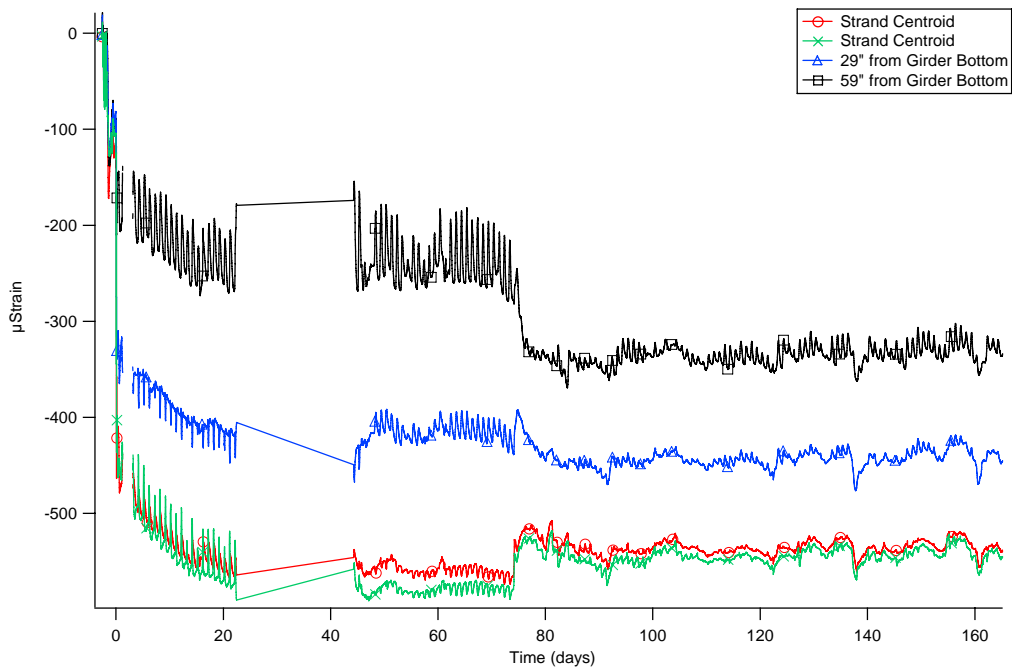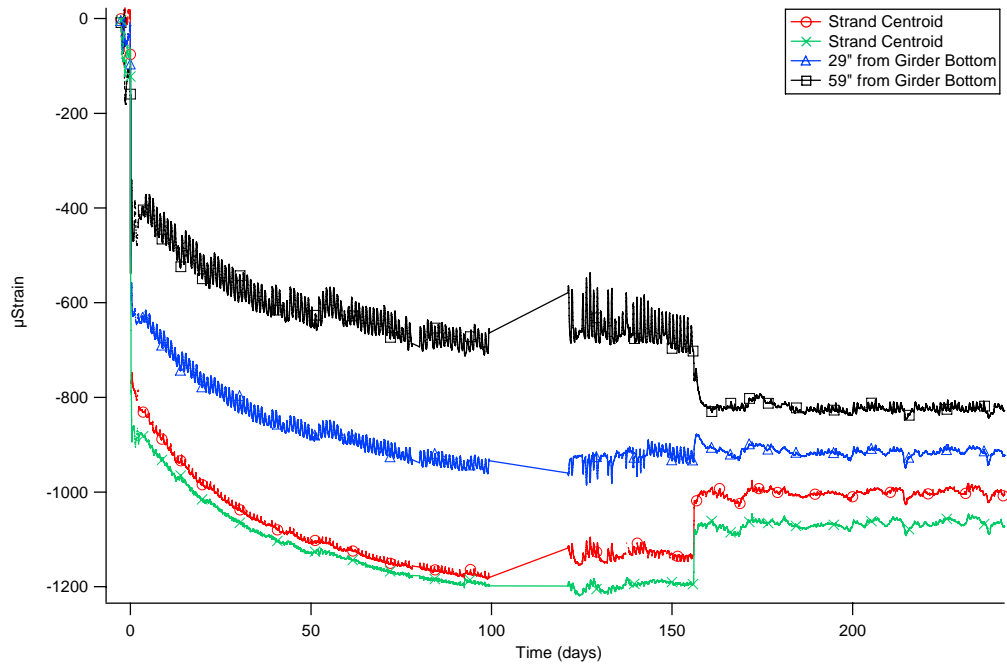
(b) 82 ft. girder

Figure 3-5 Measured strains

26
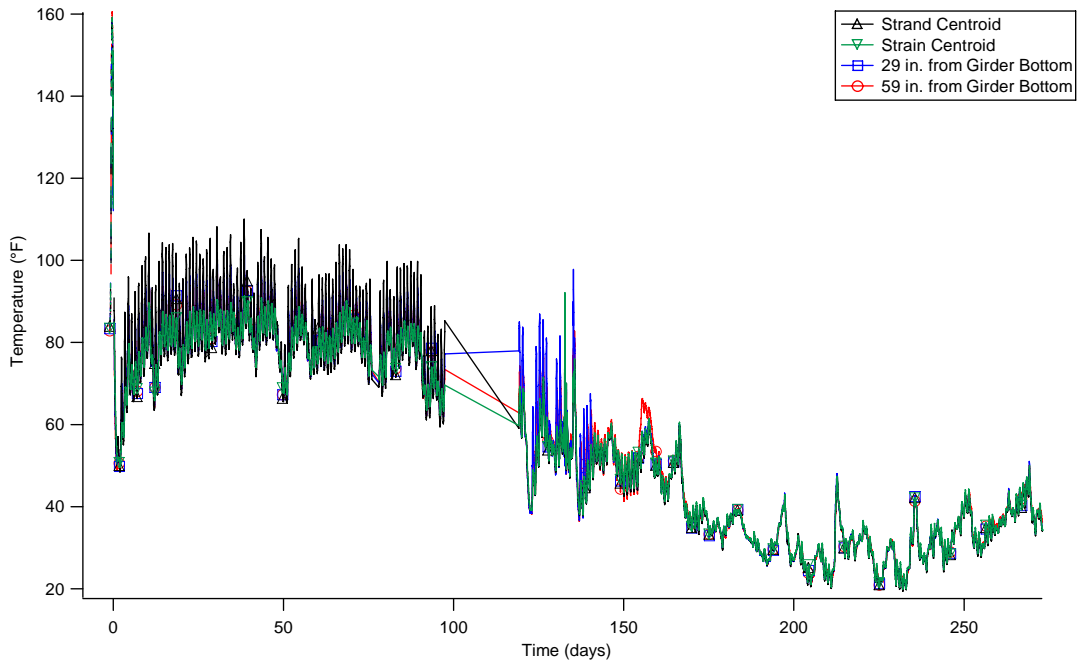
(a) Long term temperature readings
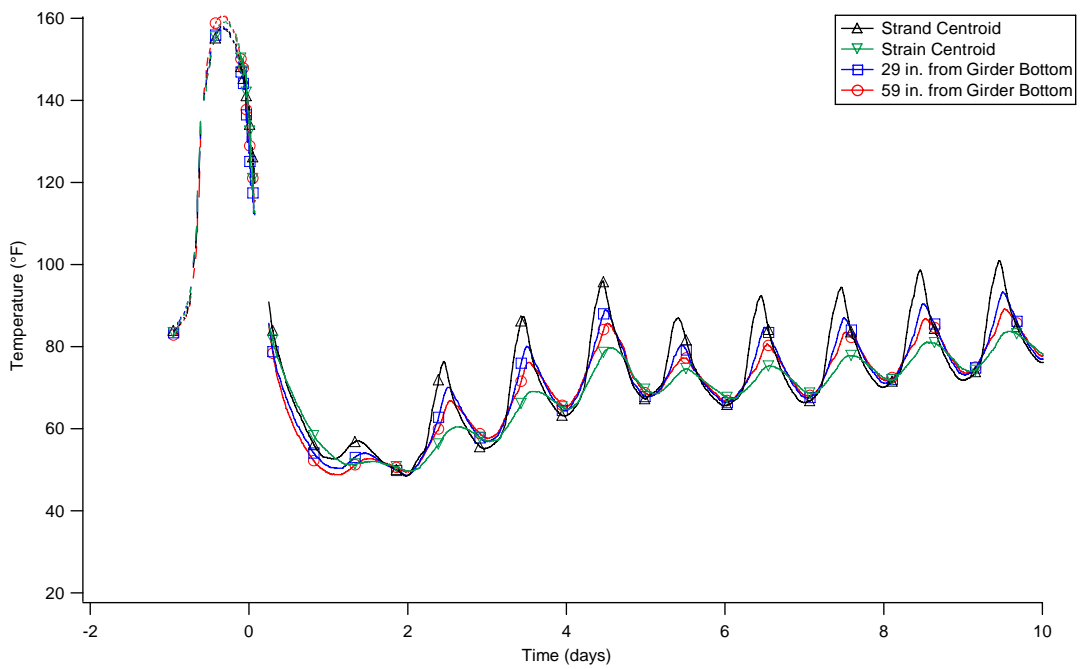
(b) Short term temperature readings

Figure 3-6 Temperature readings measured on the 132 ft. girders
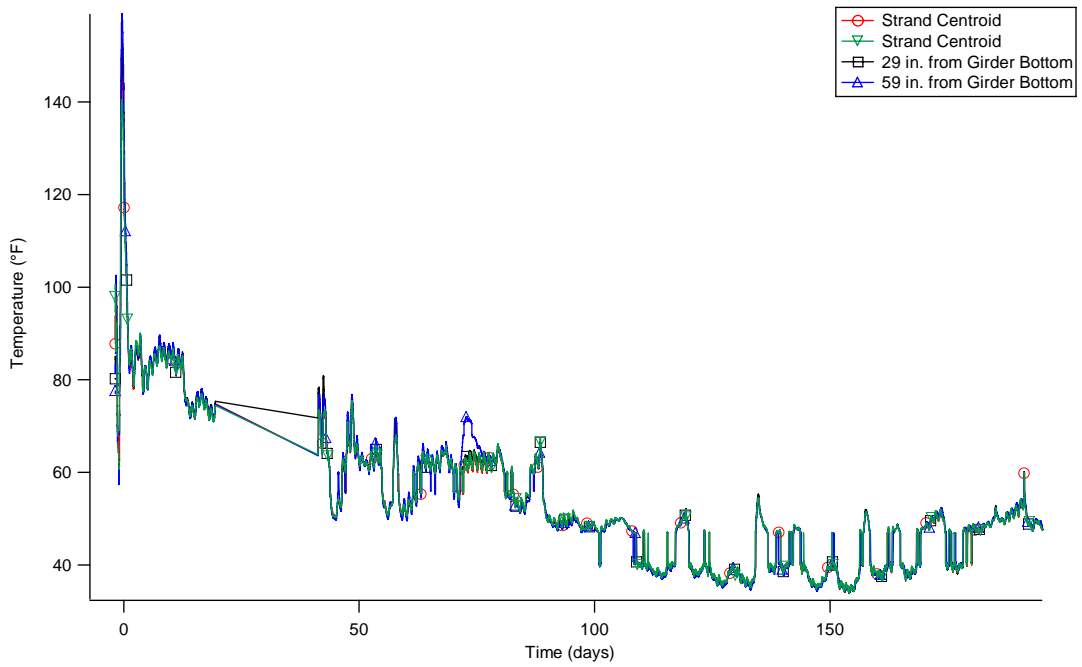
(a) Long term temperature readings
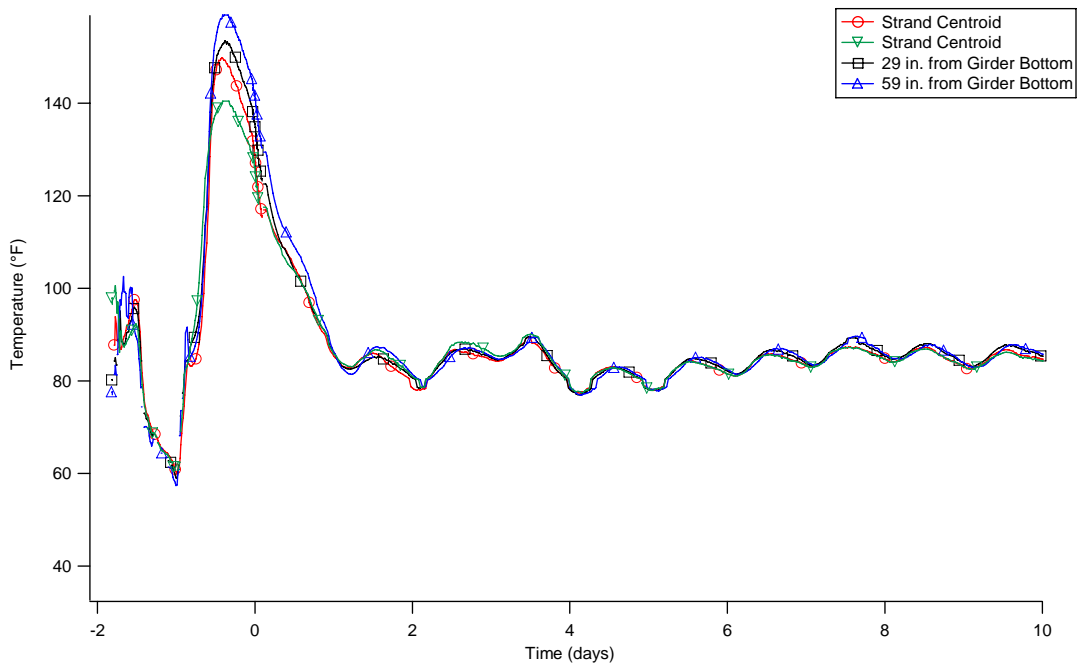
(b) Short term temperature readings

Figure 3-7 Temperature readings measured on the 82 ft. girders

28

3.3 Material Properties

The HPSCC used to fabricate the girders provided a strength and stiffness above that of conventional HPC. A representative concrete sample was taken from a front delivery concrete truck during the casting of a typical AASHTO Type VI girder. The material was sampled and specimens were made in accordance with ASTM C31 (2003), Standard Practice for Making and Curing Concrete Test Specimens in the Field. Concrete specimens included a variety of 4 in. x 8 in. and 6 in. x 12 in. cylinders and 3 in. x 17 in. beams. The 4 in. x 8 in. specimens were typically used for compressive strength measurements, while the 6 in. x 12 in. cylinders were typically used for static Young's modulus measurements. The beams were used to measure drying shrinkage.

Compressive strength and static Young's modulus measurements are presented in Table 3.1. The American Concrete Institute (ACI) committee 209 suggests Eq. (3.1) to calculate compressive strength as a function of time for moist cured concrete.

$$f_{cm} = f_{c28}\left(\frac{t}{4 + 0.85t}\right) \tag{3.1}$$

where: f_{cm} = mean compressive strength at age t days

f_{c28} = mean 28-day compressive strength

t = time in days

Compressive strength values calculated using Eq. (3.1) are presented with measured values in Fig. 3.8.

Equations suggested by ACI committee 318 (Eq. (3.2)) and the Prestressed Concrete Institute (PCI) (Eq. (3.3)) are presented along with measured values in Fig. 3.9.

$$E_s = 33000 w_c^{1.5} \sqrt{f_c'} \tag{3.2}$$

$$E_s = \left(40000\sqrt{f_c'} + 1000000\right)\left(\frac{w_c}{145}\right)^{1.5} \qquad (3.3)$$

where: E_s = static Young's modulus of elasticity

w_c = weight of concrete

f_c' = compressive strength of concrete

Measurements of shrinkage are presented in Fig. 3.10 along with values calculated using Eq. (3.4) recommended by AASHTO LRFD 2004 Specifications for moist cured concrete.

$$\varepsilon_{sh} = k_s k_h \left(\frac{t}{35+t}\right) 0.51 \times 10^{-3} \qquad (3.4)$$

where: ε_{sh} = strain due to shrinkage

k_s = size factor

k_h = humidity factor

t = drying time.

Values calculated for the estimated compressive strength using Eq. (3.1) were approximately 31.7% smaller than the measured values at day 1. This under estimation was reduced as a function of time and by day 56 the measured and calculated values correlated within 1%. This characteristic confirms previous findings that HPSCC exhibits higher strengths at early ages. This property of HPSCC makes it ideal for prestressed bridge girders due to the quick fabrication requirement.

Values of static Young's modulus calculated with Eq. (3.2) varied from approximately 29% smaller to 21% larger than the measured values on days 1 and 56, respectively. However, values of static Young's modulus calculated using Eq. (3.3) were approximately 27% smaller at day 1, but within a 2% correlation on days 7, 28, and 56. This indicates that Eq. (3.3) is more appropriate for calculations of static Young's modulus than Eq. (3.2) for this specific concrete due to the concrete's high compressive strength. HPSCC exhibits above normal properties at

young ages making it ideal for prestressed bridge girders. This comparison also shows that equations for high performance concrete can adequately be applied to HPSCC.

The shrinkage strains calculated using Eq. (3.4) were approximately 40% smaller than the average measured value at day 7 and 11% at day 56, respectively. Values presented in Fig. 3.10 exhibit that the shrinkage strain characteristics of SCC are adequately predicted by Eq. 3.4.

Table 3-1 Compressive Strength Measurements, Static Young's Modulus Measurements

Days after Casting	Load (lb.)	E_s (psi)	f'c (psi)
1	106209	4.09E+06	8452
1	103699	4.33E+06	8252
3	130759	4.58E+06	10405
3	126313	4.63E+06	10052
7	135282	4.71E+06	10765
7	147390	4.84E+06	11729
14	149990	4.65E+06	11936
14	154171	5.03E+06	12269
28	160736	5.60E+06	12791
28	161867	5.42E+06	12881
56	180397	5.63E+06	14356
56	164793	5.71E+06	13114
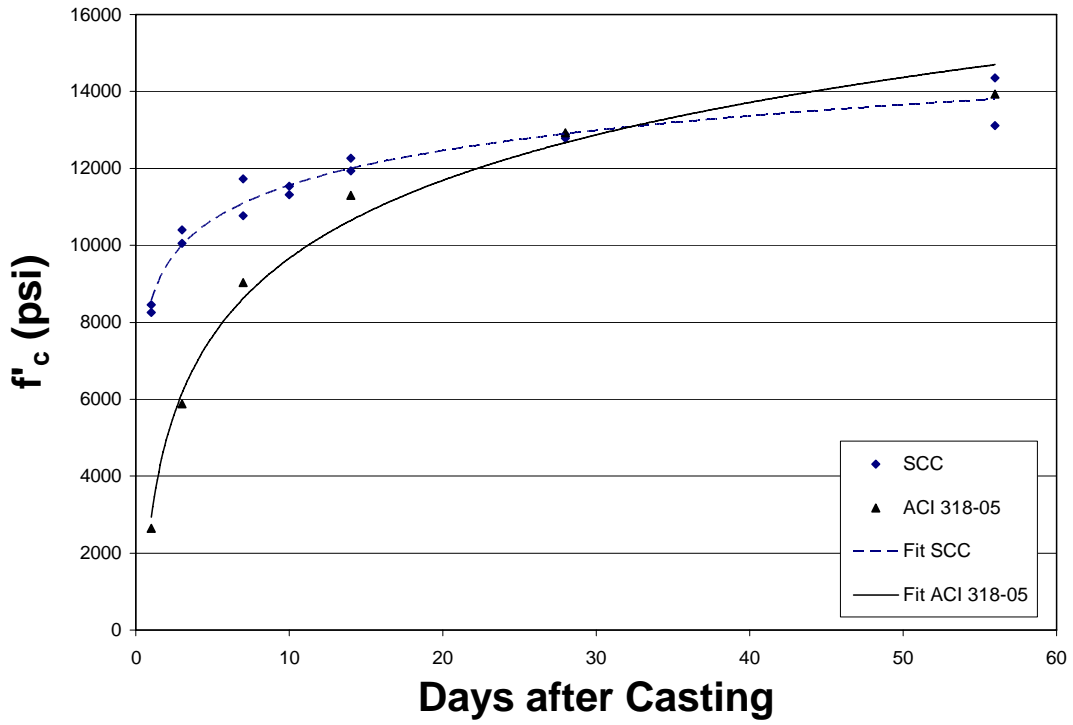
Figure 3-8 Measured and calculated compressive strength values
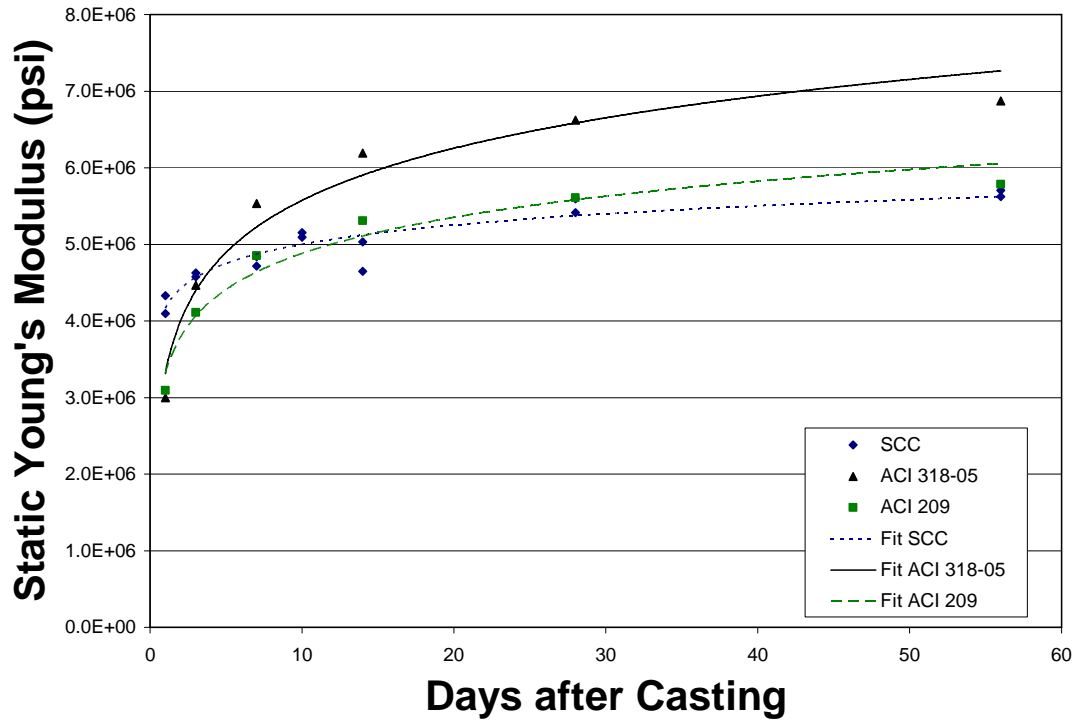
Figure 3-9 Measured and calculated static Young's modulus values
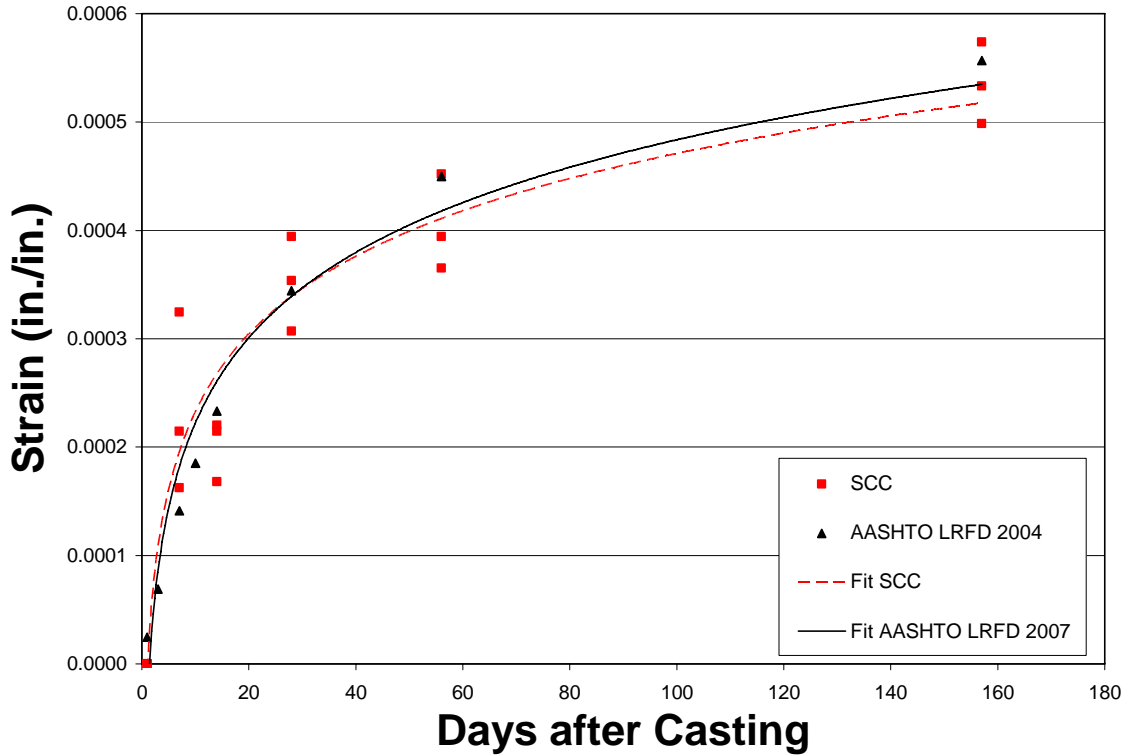
Figure 3-10 Measured and calculated shrinkage values

3.4 Total Prestress Loss

The prestressing force in a girder is lower during its service life than at initial stressing. This loss of prestress over time is due to relaxation of the prestressing steel, elastic shortening of the concrete when the prestress force is applied, creep and shrinkage of the girder, and depending on the support conditions, differential shrinkage of the deck. In addition to the reduction in stress, some stress is regained with the addition of external loads caused by superimposed loads such as the cast in place deck, concrete barriers, or sidewalks. The total prestress losses must accurately be estimated during the design of the girder so that, when subtracted from the initial jacking stress, there is sufficient remaining prestress force to provide the necessary concrete stress during service. Changes in stress due to elastic shortening, creep and shrinkage of the girder concrete, differential shrinkage of the deck, and the effects of the self weight of the deck and sidewalks were monitored for this research. The relaxation of the prestressing steel is relatively small and was not directly measured. AASHTO 2004 designates losses due to

34

relaxation as 1.2 ksi before and after transfer. AASHTO LRFD 2007 Specifications define the loss due to relaxation as approximately 2.0-4.0 ksi.

The strain measured by the VWSGs located at the centroid of the prestressing strands in each girder can be used to calculate the change in prestress (Eq. (3.5)).

$$\Delta f_{pT} = E_p \Delta \varepsilon_c \tag{3.5}$$

where: Δf_{pT} = the change in steel stress due to total prestress loss

E_p = modulus of elasticity of the prestressing steel (28,500 ksi)

$\Delta \varepsilon_c$ = measured change in strand strain

Eq. (3.5) was used with the strains measured at the centroid of the prestressing strands to calculate the total prestress losses for each of the instrumented girders. Figs. 3.11 – 3.12 present the measured prestress losses for the 132 ft. span and 82 ft. span instrumented girders, respectively.

The average measured long-term prestress losses at the last day of readings were 29.8 ksi and 16.1 ksi corresponding to approximately 14.7% and 8.0% of the initial jacking stress (202.5 ksi) for the 132 ft. and 82 ft. girders, respectively. The 82 ft. girders experienced smaller losses due to the smaller prestress force requirements. Each girder experienced a high rate of stress loss initially, but the rate of loss diminished as both a function of time, the casting of the deck, and the addition of other superimposed loads such as a sidewalk and traffic barriers. Among both the 132 ft. and 82 ft. girders, the variation in measured prestress was a maximum of 8%.

Also presented in Figs. 3.11 – 3.12 are the calculated prestress loss according the AASHTO LRFD 2004 and 2007 Specifications as well as a refined method of the 2004 Specifications using measured values of compressive strength and static Young's modulus. The lump sum method is consistent in all AASHTO LRFD Specifications and is given by Eq. (3.6). For both spans, the AASHTO LRFD 2004 predictions were higher than those made by the AASHTO LRFD 2007 Specifications. The AASHTO LRFD 2007 calculates the nearest prediction to the measured losses for both girders. However, even with the AASHTO LRFD 2007 method, the predicted total losses are still overestimated.

Figs. 3.13 – 3.14 presents the calculated prestress loss according the AASHTO LRFD 2004 and 2007 Specifications as well as a refined method of the 2004 Specifications using the specified design values of compressive strength and static Young's modulus.

Table 3.2 presents total measured and predicted losses (using measured values of compressive strength and static Young's modulus) for each of the methods at the final reading day. Also presented in Table 3.2 are values of percentage difference between the calculated values and the measured values. Similarly, Table 3.3 presents total measured and predicted losses (using specified design values of compressive strength and static Young's modulus) for each of the methods at the final reading day. Also presented in Table 3.3 are values of percentage difference between the calculated values and the measured values.

$$\Delta f_{pT} = 33 \left[1.0 - 0.15 \frac{f_c^{'} - 6.0}{6.0} \right] + 6.0 PPR \tag{3.6}$$

where: Δf_{pt} = Total loss of prestress

PPR = partial prestressing ratio

Values of prestress loss calculated using measured values of compressive strength and static Young's modulus, presented in Table 3.2, indicate that the calculated prestress losses according to the AASHTO LRFD 2007 Specifications correspond most accurately with the measured losses. For the 132 ft. girders, the AASHTO LRFD 2007 losses were 3.7% smaller. For the 82 ft. girders, the difference was 7.9%. In contrast, the AASHTO LRFD 2004 Specification calculated losses that were 76.4% and 125% overestimates of the total prestress losses measured for the 132 ft. and 82 ft. girders, respectively. Finally, using the AASHTO LRFD 2004 Refined method, calculated losses were 16.5% and 59.2% overestimates of the measured losses on the 132 ft. and 82 ft. girders, respectively.
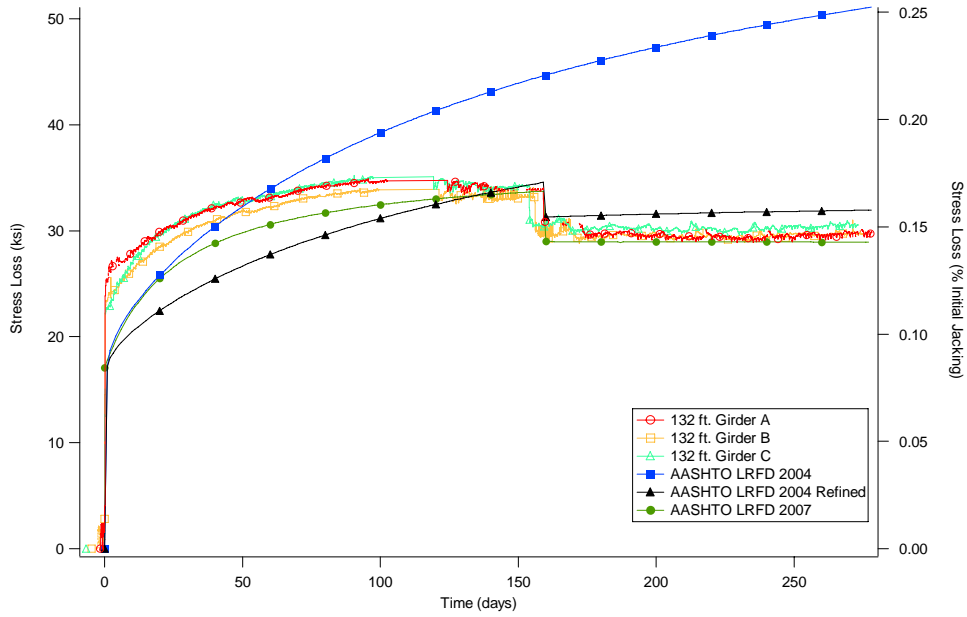
Figure 3-11 Measured and calculated (using measured values) prestress losses for the 132 ft. girders
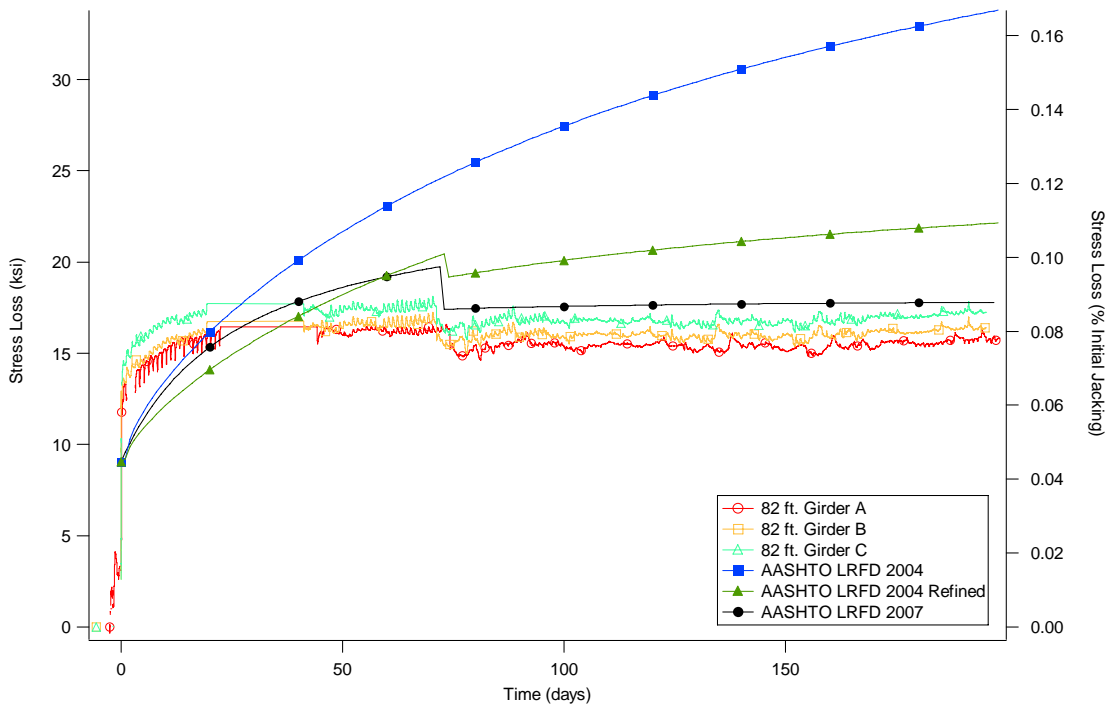
Figure 3-12 Measured and calculated (using measured values) prestress losses for the 82 ft. girders
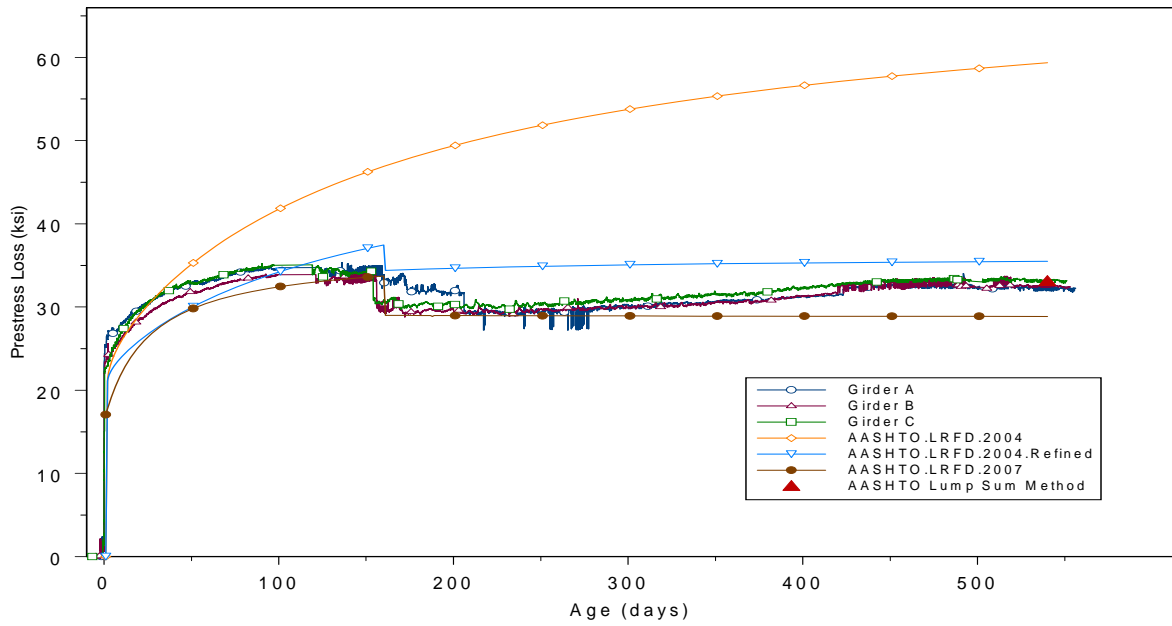
Figure 3-13 Measured and calculated (using specified values) prestress losses for the 132 ft. girders
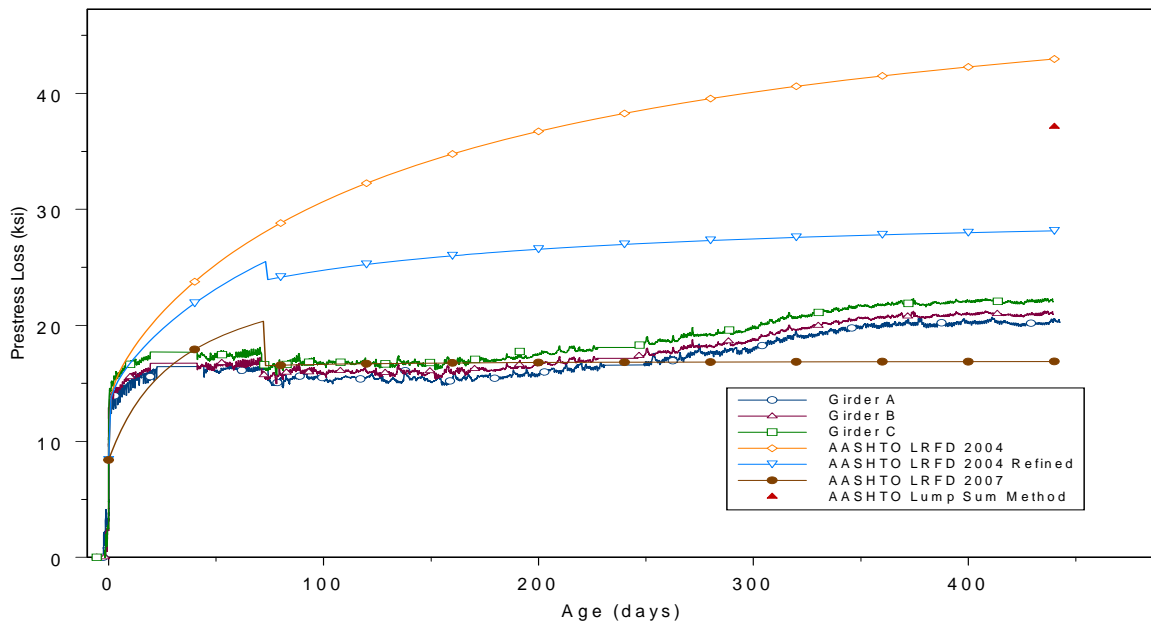
Figure 3-14 Measured and calculated (using specified values) prestress losses for the 82 ft. girders

Similarly, values of prestress loss calculated using specific design values of compressive strength and static Young's modulus, presented in Table 6.3, indicate that the AASHTO LRFD 2007 Specifications most accurately predict the values of measured losses. This method predicts prestress losses correlating within 7.6% and 1.9% of the measured values for the 132 ft. and 82 ft. girders, respectively. Calculated losses determined using the AASHTO LRFD 2004 Specifications were 68.8% and 122% overestimates of the measured losses. Finally, using the AASHTO LRFD 2004 Refined method, losses calculated were 10.3% and 60.9% overestimates of the measured losses.

These results indicate that although the specified values of compressive strength static Young's modulus were lower than the measured values, all of the methods used to calculate prestress losses produced consistent results. The largest difference was found using the AASHTO LRFD 2007 Specifications. For the 132 ft. girders, values calculated using the measured values and specified design values were 3.7% smaller and 7.6% larger than the measured losses, respectively. This represents a difference of only 1.18 ksi.

In order to investigate the discrepancies, the measured and predicted prestress loss components (elastic shortening, creep and shrinkage, and differential shrinkage) were compared.

Table 3-2 Total Calculated (using Measured Values) and Measured Prestress Losses for the (a) 132 ft. and (b) 82 ft. Girders

(a)

	Prestress Loss (% Initial Jacking)	Percent Difference
AASHTO LRFD Lump Sum	0.16	10%
AASHTO LRFD 2004	0.26	76%
AASHTO LRFD 2004 Refined	0.17	17%
AASHTO 2007 Simplified	0.18	24%
AASHTO 2007 Refined	0.14	-4%
Average Measured Data	0.15	

(b)

	Prestress Loss (% Initial Jacking)	Percent Difference
AASHTO LRFD Lump Sum	0.16	99%
AASHTO LRFD 2004	0.18	125%
AASHTO LRFD 2004 Refined	0.13	59%
AASHTO 2007 Simplified	0.11	39%
AASHTO 2007 Refined	0.09	8%
Average Measured Data	0.08	

Table 3-3 Total Calculated (using Specified Values) and Measured Prestress Losses for the (a) 132 ft. and (b) 82 ft. Girders

(a)

	Prestress Loss (% Initial Jacking)	Percent Difference
AASHTO LRFD Lump Sum	0.19	25%
AASHTO LRFD 2004	0.25	69%
AASHTO LRFD 2004 Refined	0.16	10%
AASHTO 2007 Simplified	0.20	35%
AASHTO 2007 Refined	0.14	-8%
AASHTO LUMP Sum	0.16	6%
Average Measured Data	0.15	

(b)

	Prestress Loss (% Initial Jacking)	Percent Difference
AASHTO LRFD Lump Sum	0.18	125%
AASHTO LRFD 2004	0.18	122%
AASHTO LRFD 2004 Refined	0.13	61%
AASHTO 2007 Simplified	0.11	39%
AASHTO 2007 Refined	0.08	2%
AASHTO Lump Sum	0.16	100%
Average Measured Data	0.08	

3.5 Elastic Shortening

After the concrete has gained sufficient strength in the casting bed, the forms are removed and the prestressing strands are released. As the prestressing force is transferred to the concrete, the girder axially shortens and cambers due to the prestressing force. Because the strands are now bonded to the concrete, they also shorten and lose a portion of the initial jacking prestressing force. This loss of prestressing force at release is termed elastic shortening loss and can be a significant portion of the total loss of force.

The AASHTO LRFD 2004 and 2007 Specifications present the same two formulas for the calculation of the loss due to elastic shortening:

$$\Delta f_{pES} = \frac{E_p}{E_{ci}} f_{cgp} \tag{3.7}$$

$$\Delta f_{pES} = \frac{A_{ps} f_{pbt}(I_g + e_m^2 A_g) - e_m M_g A_g}{A_{ps}(I_g + e_m^2 A_g) + \frac{A_g I_g E_{ci}}{E_p}} \tag{3.8}$$

where: Δf_{pES} = elastic shortening

E_p = modulus of elasticity of prestressing steel

E_{ci} = modulus of elasticity of concrete at transfer

f_{cgp} = sum of concrete stresses at the center of gravity of prestressing tendons due to the prestressing force at transfer and the self-weight of the member at the sections of maximum moment

A_{ps} = area of prestressing steel

A_g = gross area of section

e_m = average eccentricity at midspan

f_{pbt} = stress in prestressing steel immediately prior to transfer

I_g = moment of inertia of the gross concrete section

M_g = midspan moment due to member self-weight

When determining the prestress loss due to elastic shortening at midspan, either Eq (3.7) or Eq. (3.8) can be used. However, when a more detailed analysis of a specific section of a girder is required, Eq. (3.7) may be used at each section along the beam, in places where loading conditions may differ.

The values calculated for elastic shortening using the measured elastic modulus (Fig. 3.9) in Eqs. (3.7 – 3.8), and the average values measured on the 132 ft. and 82 ft. girders are presented in Fig. 3.15.

The average measured losses due to elastic shortening were 18.33 ksi, 19.16 ksi, and 16.57 ksi for 132 ft. girders A, B, and C and 8.48 ksi, 10.02 ksi, and 8.98 ksi for 82 ft. girders A, B, and C, respectively. The calculated values for elastic shortening were 17.07 ksi and 9.05 ksi, and correlated to the measured values by 93%, 89%, and 103%, and 94%, 111%, and 99%, respectively. The measured and calculated losses represent 9.1%, 9.5%, and 8.2%, and 4.4%, 4.9%, and 4.4% of the initial jacking stress for the 132 ft. girders A, B, and C, and the 82 ft. girders A, B, and C, respectively.

Also, Eq. (3.2) was used to determine a calculated value of modulus of elasticity. Using this value, the calculated values for prestress loss due elastic shortening for the 132 ft. and 82 ft. girders were 16.0 and 8.4 ksi, respectively. The calculated values for elastic shortening using the calculated value of elastic modulus correlated to the measured values by 114%, 120%, and 104%, and 101%, 119%, and 107%, for the 132 ft. girders A, B, and C, and the 82 ft. girders A, B, and C, respectively.

The results indicate that the measured and calculated values of elastic moduli were very similar, and in fact this was found to be true. The measured value of static Young's modulus at day 1 was an average of 4.21×10^6 psi (Table 3.1) and the value calculated using Eq. (3.2) was 4.6×10^6 psi. The static Young's modulus determined using Eq. (3.3) was not used in the calculation of elastic shortening because it is not suggested by any of the AASHTO LRFD Specifications.

On average, the measured value of elastic modulus was a better indicator of prestress loss due to elastic shortening.
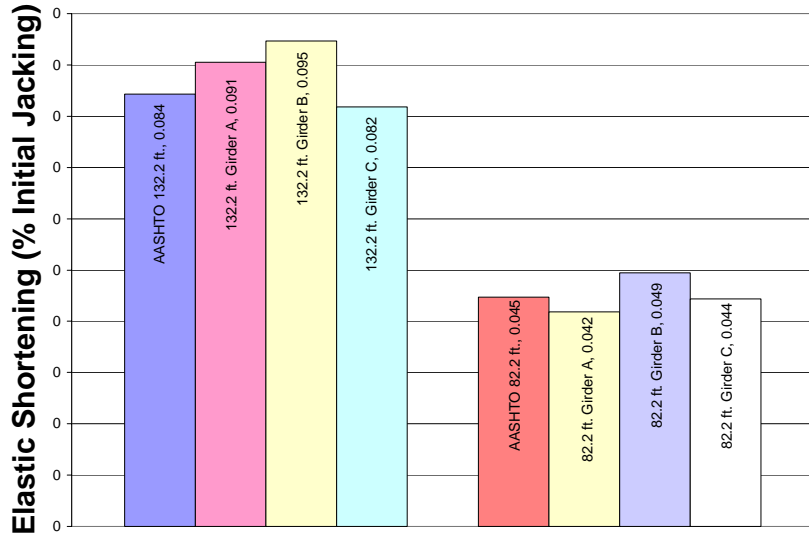
Figure 3-15 Measured and calculated prestress losses due to elastic shortening

3.6 Creep and Shrinkage

Creep is defined as an increase in strain as a function of time due to a constant stress. In the case of concrete, the constant stress is due to prestress force, self weight, and superimposed dead loads. Thus, concrete creep is a time-dependent flow caused by its subjection to stress. This deformation occurs rapidly at first and then decreases with time, and, in prestressed concrete girders, can be several times larger than the deformation due to elastic shortening. Creep has been found to depend on mix proportions, humidity, curing conditions, and maturity of the concrete when first loaded (Neville 1995). The creep deformation causes a change of the prestressing strand strain, which changes the strand stress.

There are two types of shrinkage that affects the girder concrete, basic and drying shrinkage. Basic shrinkage is caused by the hydration of the cement as the concrete cures and is independent of the volume or surface of the concrete structure. The evaporation of excess water during curing is the cause of drying shrinkage. Drying shrinkage is unrelated to load application or thermal effects. The amount of water contained in most concrete mixes is more than is needed for the complete hydration of the cementitious materials. This excess water leaches to the surface and evaporates as a function of time. As the excess water makes it to the surface and

evaporates the concrete structure is reduced in volume. The rate of volume reduction occurs initially at a high rate and later diminishes with time. This is due to both the lack of excess water and increase in stiffness as the concrete cures. Shrinkage is affected by many parameters, including mix proportions, type of aggregate, cement type, time between the end of external curing and the application of loading, and environmental conditions (Neville 1995). As was the case for creep, shrinkage of the concrete causes shortening of the prestressing strands which reduces the prestressing force.

The measured change in strain in the prestressing strands due to creep and shrinkage was computed by subtracting the measured strain due to elastic shortening from the average measured change in strain at the prestressing centroid as a function of time. Corresponding values of creep and shrinkage were also calculated using the AASHTO LRFD 2004, 2004 Refined, and 2007 Specifications.

The AASHTO LRFD 2004 Specification defines the prestress losses due to creep and shrinkage as:

$$\Delta f_{pCR} = 12.0 f_{cgp} - 7.0 \Delta f_{cdp} \geq 0 \tag{3.9}$$

$$\Delta f_{pSR} = (17.0 - 0.15H) \tag{3.10}$$

where: Δf_{pCR} = prestress loss due to creep

Δf_{cdp} = change in concrete stress at center of gravity of prestressing steel due to permanent loads, with the exception of the load acting at the time the prestressing force is applied

Δf_{pSR} = prestress loss due to shrinkage

H = the average annual ambient relative humidity

The AASHTO 2004 Refined method specifies the prestress losses due to creep and shrinkage as:

$$\Delta f_{pCR} = \eta_{CR,TR}(t, t_{i,TR}) f_{cgp} - \eta_{CR,LT}(t, t_{i,LT}) \Delta f_{cdp} \tag{3.11}$$

$$\Delta f_{pSR} = E_p \varepsilon_{SH} \tag{3.12}$$

$$\varepsilon_{SH} = -k_s k_h \left(\frac{t}{35+t} \right) 0.51 \times 10^{-3} \tag{3.13}$$

44

where: $\eta_{CR,TR}$ = creep modular ratio at transfer

t = time

$t_{i,TR}$ = age of concrete at transfer

$\eta_{CR,LT}$ = creep modular ratio for permanent loads

$t_{i,LT}$ = age of concrete when permanent loads are applied

ε_{SH} = strain due to shrinkage at time, t

k_s = factor for the effect of the volume to surface ratio

k_h = humidity factor.

Finally, the AASHTO LRFD 2007 Specifications define prestress losses due to creep and shrinkage as:

$$\Delta f_{pCR} = \frac{E_p}{E_{ci}} f_{cgp} \psi_b (t_d, t_i) K_{id} \tag{3.14}$$

$$\Delta f_{pSR} = \varepsilon_{bid} E_p K_{id} \tag{3.15}$$

where: $\psi_b(t_d, t_i)$ = girder creep coefficient at time of deck placement due to loading

introduced at transfer

K_{id} = transformed section coefficient that accounts for time dependent interaction

between concrete and bonded steel in the section being considered for time period

between transfer and deck placement

ε_{bid} = concrete shrinkage strain of girder between the time of transfer and deck

placement

The calculated values of prestress loss due to creep and shrinkage are overestimated by nearly all design specifications (Fig. 3.16, Tables 3.4 – 3.5). The AASHTO LRFD 2007 Specifications did the best job and predicted the losses due to

shrinkage and creep for the 132 ft. and 82 ft. girders within 1.3% and 19.3%, respectively. This discrepancy is mostly likely due to the irregularly high values of compressive strength and modulus of elasticity. The AASHTO LRFD 2004 and 2004 Refined Specifications are based on conventional strength concrete which is believed to have larger creep and shrinkage losses. Although the AASHTO LRFD 2007 Specifications include methodologies to incorporate HPC, the measured values of compressive strength and modulus of elasticity of the HPSCC used are higher than those typically recognized for HPC. This may be the cause for the over prediction of prestress loss due to creep and shrinkage by the AASHTO LRFD 2007 Specifications. Also, Fig. 3.10 presents a close correlation between the shrinkage strain of HPSCC concrete specimen and the values calculated using AASHTO LRFD Specifications. This close correlation between measured and calculated strains due to shrinkage indicates that the discrepancies found in the creep and shrinkage prestress loss predictions may be due mostly to creep.

3.7 Deck Casting

AASHTO LRFD 2004 Refined and 2007 Specifications include provisions to include the prestress gains during deck placement. The values calculated by these two codes are presented along with measured values in Fig. 3.17. Fig. 3.17 shows that, excluding the 132 ft. girder A, the values predicted by both codes correlate within 10% for the 132 ft. girders and 15% for the 82 ft. girders. The AASHTO LRFD 2004 Refined method provides this additional prestress through changes in creep induced loads calculated using Eq. (3.11). The AASHTO LRFD 2007 Specifications suggest formulas to predict prestress losses from both shrinkage and creep between the time of deck placement and final time, Eqs. (3.16 and 3.17, respectively).

$$\Delta f_{pSD} = \varepsilon_{bdf} E_p K_{df} \tag{3.16}$$

$$\Delta f_{pCD} = \frac{E_p}{E_{ci}} f_{cgp} \psi_b \left[\left(t_f, t_i \right) - \psi_b \left(t_d, t_i \right) \right] K_{df} + \frac{E_p}{E_c} \Delta f_{cd} \psi_b \left(t_f, t_d \right) K_{df} \tag{3.17}$$

where: ε_{bdf} = shrinkage strain of girder between the time of deck placement and final time

K_{df} = transformed section coefficient that accounts for time-dependent interaction between concrete and bonded steel in the section being considered for time period between deck placement and final time

$\psi_b(t_f,t_i)$ = girder creep coefficient at final time due to loading introduced at transfer

f_{cd} = change in concrete stress at centroid of prestressing strands due to shrinkage of deck concrete

$\psi_b(t_f,t_d)$ = girder creep coefficient at final time due to loading at deck placement

Overall, the values of prestress gain due to the deck placement represent only a small component of the overall losses. Also, the measured gains may be smaller than the actual gains due to the boundary conditions of the girders (i.e. they are restrained at the abutments). Finally, the load induced to the exterior girders due to their larger tributary areas would cause a larger gain than measured on the interior girders.
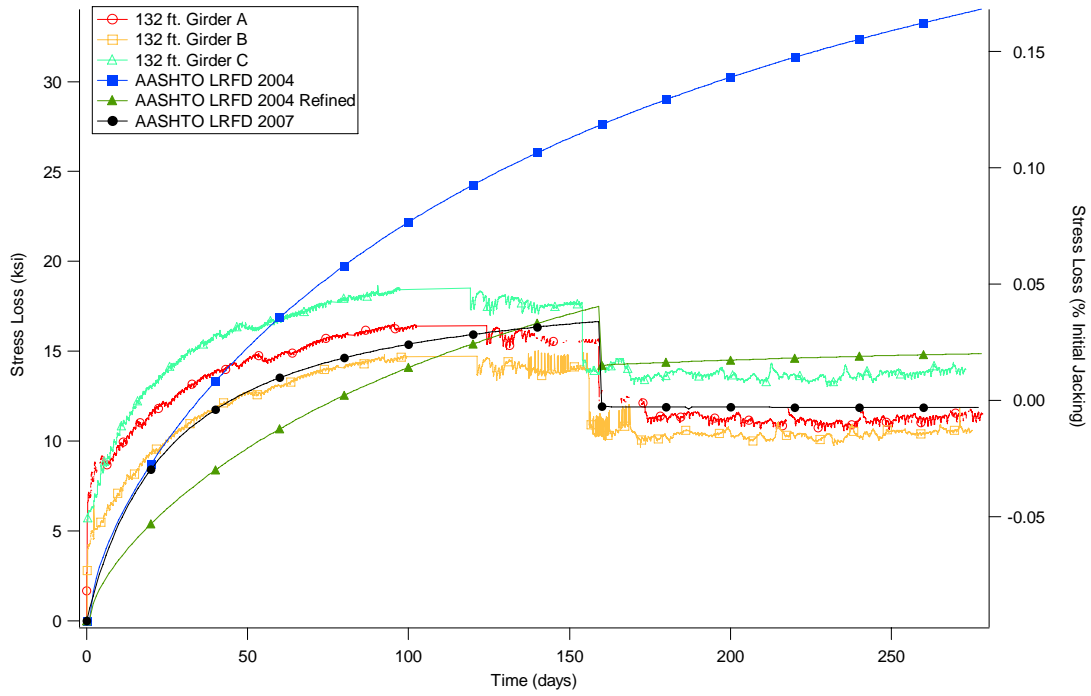
(a) 132 ft. girder
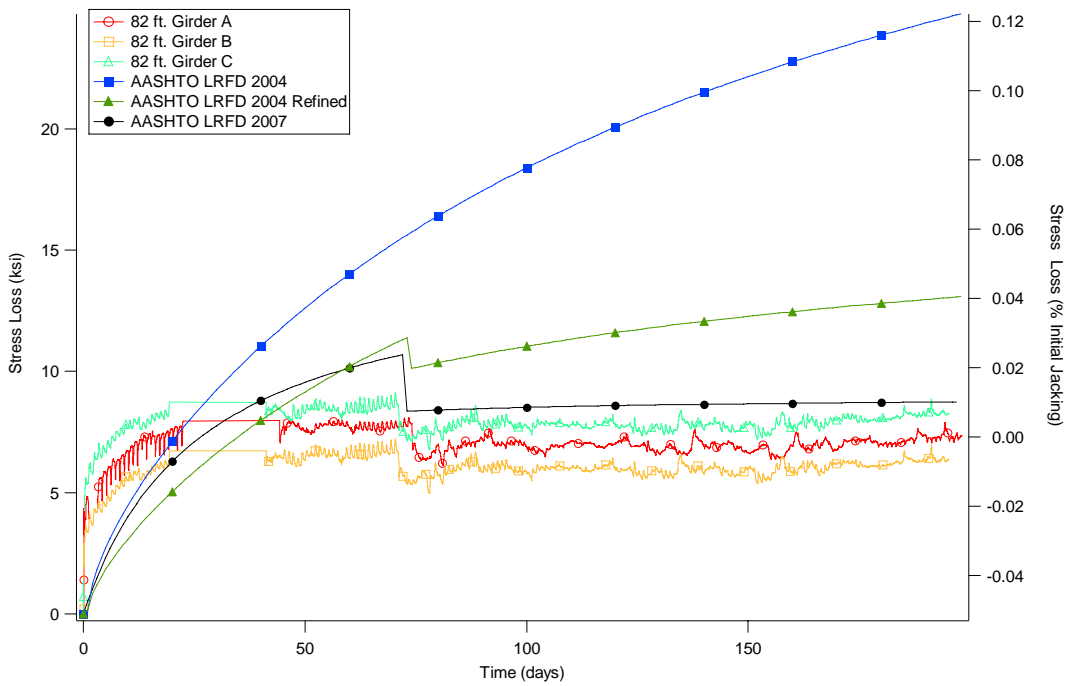
(b) 82 ft. girder

Figure 3-16 Measured and calculated (using measured values) prestress losses due to creep and shrinkage

48

Table 3-4 Calculated and Measured Prestress Losses Due to Creep and Shrinkage for the (a) 132 ft. and (b) 82 ft. Girders Using Measured Values of static Young's Modulus

(a)

	Prestress Loss (% Initial Jacking)	Percent Difference
AASHTO LRFD 2004	0.18	199%
AASHTO LRFD 2004 Refined	0.09	49%
AASHTO 2007 Refined	0.06	-1%
Average Measured Data	0.06	

(b)

	Prestress Loss (% Initial Jacking)	Percent Difference
AASHTO LRFD 2004	0.138	282%
AASHTO LRFD 2004 Refined	0.085	135%
AASHTO 2007 Refined	0.043	19%
Average Measured Data	0.036	

Table 3-5 Calculated and Measured Prestress Losses Due to Creep and Shrinkage for the (a) 132 ft. and (b) 82 ft. Girders Using Specified Values of Static Young's Modulus

(a)

	Prestress Loss (% Initial Jacking)	Percent Difference
AASHTO LRFD 2004	0.171	189%
AASHTO LRFD 2004 Refined	0.085	43%
AASHTO 2007 Refined	0.058	-2%
Average Measured Data	0.059	

(b)

	Prestress Loss (% Initial Jacking)	Percent Difference
AASHTO LRFD 2004	0.140	286%
AASHTO LRFD 2004 Refined	0.090	148%
AASHTO 2007 Refined	0.042	15%
Average Measured Data	0.036	
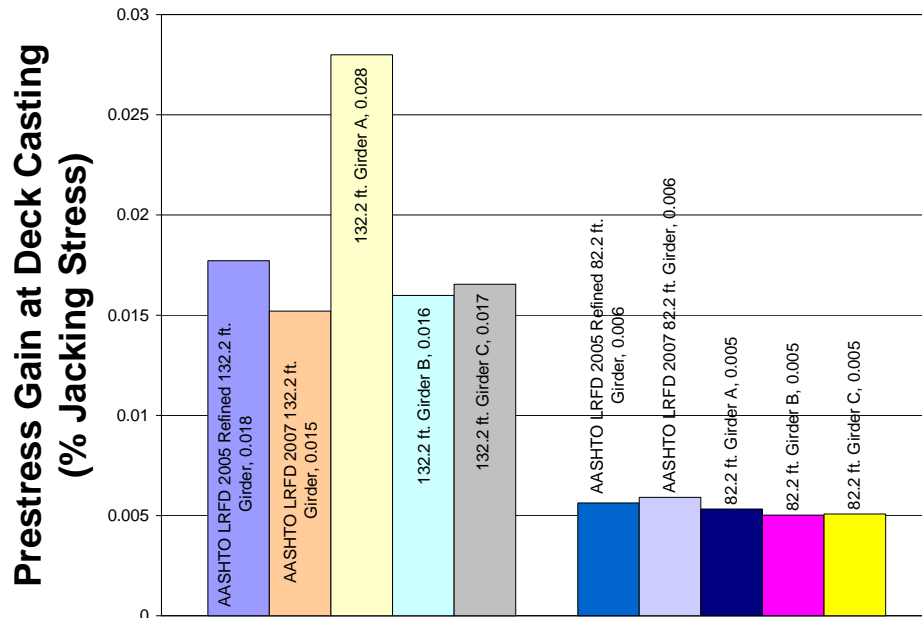
Figure 3-17 Measured and calculated prestress gains at deck placement

3.8 Differential Shrinkage

One explanation as to why the calculated AASHTO LRFD 2007 creep and shrinkage losses were lower than those calculated by the AASHTO LRFD 2004 and 2004 Refined Specifications can be explained by comparing the differential shrinkage losses. Stress loss due to shrinkage of composite, prestressed concrete girders comes from two sources. The first source is the shrinkage of the girder concrete. The second source is the shrinkage of the deck concrete. The deck concrete is typically placed several months after the girder concrete has been cast. Thus, the rate of creep and shrinkage of the girder concrete has decreased by the time the deck is placed. However, the deck concrete has yet to experience its shrinkage. The effect of differences between the shrinkage strain of the deck concrete and the shrinkage strain of the girder concrete is termed differential shrinkage.

The AASHTO LRFD 2004 and 2004 Refined Specifications do not explicitly take into account differential shrinkage in its calculations of changes prestress. The AASHTO LRFD 2007 Specifications does include differential shrinkage. The change in stress due to differential shrinkage can be calculated as:

$$\Delta f_{pSS} = \frac{E_p}{E_c} \Delta f_{cdf} K_{df} \left[1 + 0.7 \psi_d (t_f, t_d) \right] \qquad (3.16)$$

where: Δf_{pSS} = the prestress gain due to shrinkage of deck composite section

Δf_{cdf} = change in concrete stress at centroid of prestressing strands due to shrinkage of deck concrete

K_{df} = transformed section coefficient that accounts for time dependent interaction between concrete and bonded steel in the section being considered for time period between deck placement and final time

$\psi_d(t_f, t_d)$ = creep coefficient of deck concrete at final time due to loading introduced shortly after deck placement (i.e. overlays, barriers, etc.)

Values calculated for prestress loss due to differential shrinkage of the 132 ft. and 82 ft. girders were 2.70 ksi and 1.80 ksi, respectively using the measured values of elastic modulus and compressive strength. The values grew to 4.16 and 3.24, respectively, when the specified values were used. This is due to the fact that the specified values were lower than the measured values, thus increasing strains and prestress loss due to differential shrinkage. Fig. 3.18 presents average measured values of the 132 ft. and 82 ft. girders along with values of prestress loss due to differential shrinkage calculated using the AASHTO LRFD 2007 Specifications. Values were calculated and are presented using both measured and specified static Young's moduli and compressive strengths.

Fig. 3.18 shows that from the time of deck placement to final time, values of prestress loss due to differential shrinkage do an adequate job of predicting the behavior for both the 132 ft. and 82 ft. girders. However, there is a great deal of scatter in the

51

measured values probably due to temperature induced stress changes and traffic. Thus, it is difficult to measure exactly which calculated value best predicts the measured behavior. However, the calculated values of differential shrinkage determined using specified values of elastic moduli and compressive strength appears to provides a closer fit for the 132 ft. girder. In contrast, the calculated values of differential shrinkage determined using measured values of elastic moduli and compressive strength appears to provides a closer fit for the 82 ft. girder
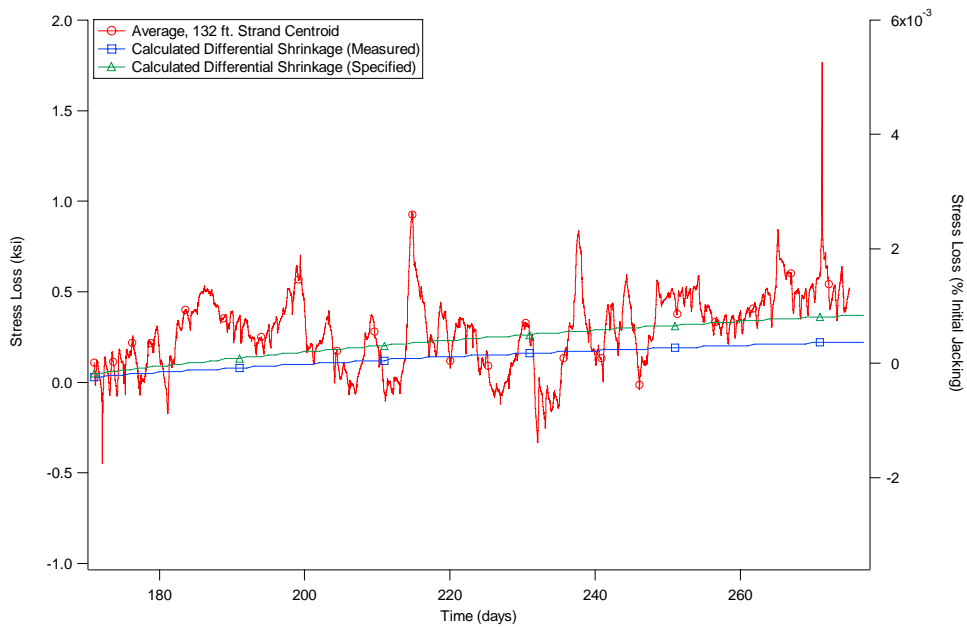
(a) 132 ft. girder

(b) 82 ft. girder
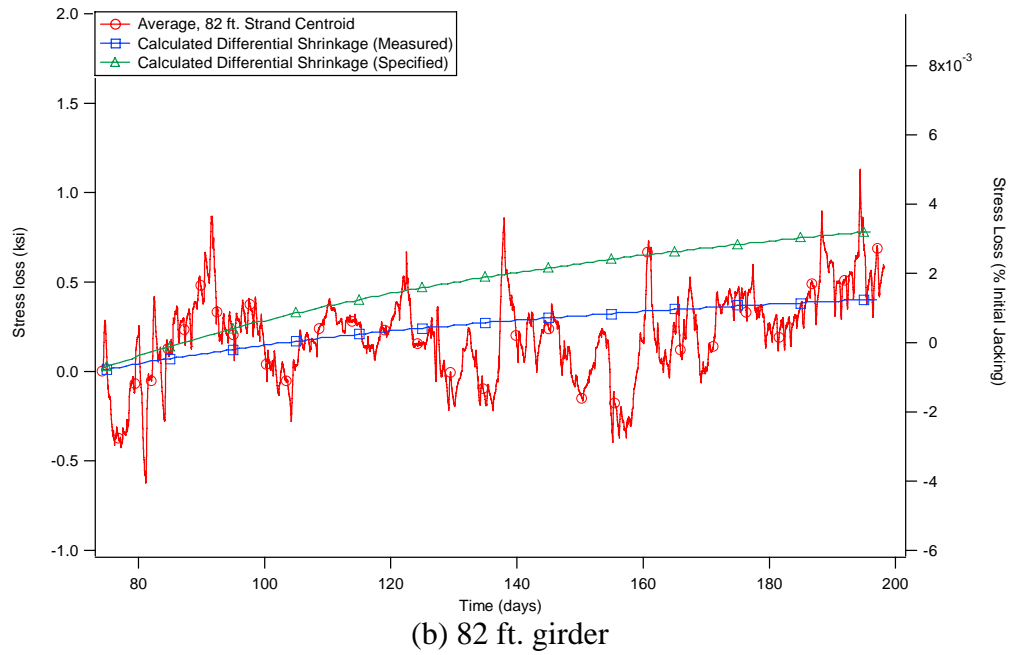
Figure 3-18 Measured and calculated prestress losses due to differential shrinkage

CHAPTER 4 CONCLUSIONS, RECOMMENDATIONS/IMPLEMENTATIONS

This study describes the measured behavior of six, high performance, self-consolidating concrete (HPSCC), prestressed bridge girders using embedded vibrating wire strain gages (VWSG). Measurements were made on material specimens of the HPSCC used to make the bridge girders. The measured strains for the VWSGs were used to determine prestress losses that were compared to calculated values obtained using the 2004 and 2007 AASHTO LRFD Specifications. The study led to the following conclusions and recommendations:

1. Values calculated for the compressive strength using ACI 318-05 (Eq. (1) in this study) were approximately 31.7% smaller than the measured values at day 1. This under estimation grew smaller as a function of time and by day 56 the measured and calculated values correlated within 1%. Values of static Young's modulus calculated with ACI 318-05 (Eq. (2) in this study) varied from approximately 29% smaller to 21% larger than the measured values on days 1 and 56, respectively. However, values of static Young's modulus calculated using the equation suggested by ACI committee 209 (Eq. (6.3) in this study) were approximately 27% smaller at day 1, but within a 2% correlation on days 7, 28, and 56. Shrinkage strains calculated in accordance with AASTHO LRFD Specifications (Eq. (6.4) in this study) were approximately 40% smaller than the average measured value at day 7 and 1% and 11% at days 28 and 56, respectively.

54

2. The average measured prestress losses after the deck was cast were 29.8 ksi and 16.1 ksi corresponding to approximately 14.7% and 8.0% of the initial jacking stress of 202.5 ksi for the 132 ft. and 82 ft. girders, respectively.

3. Among both the 132 ft. and 82 ft. girders, the variation in measured prestress was a maximum of 8%.

4. AASHTO LRFD 2007 Specifications predicted the total prestress loss within 3.7% and 7.9% for the 132 ft. and 82 ft. girders, respectively. In contrast, the predictions calculated using the AASHTO LRFD 2004 Specification were 76.4% and 125% overestimates of the total prestress losses measured for the 132 ft. and 82 ft. girders, respectively. Finally, the AASHTO LRFD 2004 Refined method predicted losses within 16.5% and 59.2% of the measured losses for the 132 ft. and 82 ft. girders, respectively

5. Values of prestress loss due to elastic shortening determined using the AASHTO LRFD 2007 Specifications were within 7.0% and 6.2% for the 132 ft. and 82 ft. girders, respectively.

6. The calculated values of prestress loss due to creep and shrinkage calculated using the AASHTO LRFD 2007 Specifications predicted the losses due to shrinkage and creep for the 132 ft. and 82 ft. girders most accurately within 1.3% and 19.3%, respectively.

7. This study shows that design practices are improving, and that prestress losses for high strength self-consolidating concrete can be predicted with them.

8. The largest discrepancies between measured and predicted prestress loss values were due to calculated values of creep and shrinkage. Future AASHTO LRFD Specifications should continue to develop more appropriate equations for the calculation of these values for HPC.

REFERENCES

Ahlborn, T.M.; French, C.E.; and Leon, R.T., 1995, Applications of High-Strength Concrete to Long-Span Prestressed Bridge Girders, Transportation Research Record, No. 1476, pp. 22-30.

American Association of State Highway and Transportation Officials (AASHTO), 1989, Standard Specifications for Highway Bridges, 14th Edition, Washington, D.C.

American Association of State Highway and Transportation Officials (AASHTO), 2004, LRFD Bridge Design Specifications, 3rd Edition, Washington, D.C.

American Association of State Highway and Transportation Officials (AASHTO), 2007, LRFD Bridge Design Specifications, 4th Edition, Washington, D.C.

American Standard for Testing and Materials, ASTM C 469, 2002, Standard Test Method for Static Modulus of Elasticity and Poisson's Ratio of Concrete in Compression, ASTM International, West Conshohocken, PA.

American Standard for Testing and Materials, ASTM C 1611, 2005, Standard Test Method for Slump Flow of Self Consolidating Concrete, ASTM International, West Conshohocken, PA.

American Standard for Testing and Materials, ASTM C 31, 2003, Standard Practice for Making and Curing Concrete Test Specimens in the Field, ASTM International, West Conshohocken, PA.

Barr, P.J.; Kukay, B..M.; and Halling, M.W., 2007, Comparison of Prestress Losses for a Prestress Concrete Bridge Made with High Performance Concrete.

Cole, H. A., 2000, Direct Solution for Elastic Prestress Loss in Pretensioned Concrete Girders, Practice Periodical on Structural Design and Construction, Vol. 5, pp. 27-31.

Gilbertson, C. G., and Ahlborn, T. M., 2004, A Probabilistic Comparison of Prestress Loss Methods in Prestressed Concrete Beams, PCI Journal, pp. 52-69.

Gross, S.P., 1999, Field Performance of Prestressed High Performance Concrete Highway Bridges in Texas, Ph.D. Dissertation, The University of Texas at Austin.

Kowalsky, M.J.; Zia, P.; Wagner, M.C.; and Warren, B.A., 2001, The Behavior of Prestressed High Performance Concrete Bridge Girders for US Highway 401 over the Neuse River in Raleigh, NC, Federal Highway Administration Research Report 23241-97-8, Washington, D.C.

Kukay, B.; Barr, P. J.; and Halling, M.W., 2007, A Comparison of Time Dependent Prestress
Losses in a Two-Span, Prestressed Concrete Bridge.

Neville, A. M., 1995, Properties of Concrete, 4th ed., Pearson Education Limited.

Roller, J. J.; Russell, H. G.; Bruce, R. N.; and Martin, B. T., 1995, Long-Term Performance
of Prestressed, Pretensioned High Strength Concrete Bridge Girders, PCI Journal, Vol.
43, No. 6, pp. 48-58.

Stallings, M. J.; Barnes, R. W.; and Eskildsen, S., 2003, Camber and Prestress Losses in
Alabama HPC Bridge Girders, PCI Journal.

Tadros, M.K.; Al-Omaishi, N.; Seguirant, S.J.; and Gallt, J.G., 2003, Prestress Losses in
Pretensioned High-Strength Concrete Bridge Girders. NCHRP Report 496, National
Cooperative Highway Research Program, Transportation Research Board, National
Research Council.

Yang, Y., and Myers, J. J., 2005, Prestress Loss Measurements in Missouri's First Fully
Instrumented High-Performance Concrete Bridge, Transportation Research Record:
Journal of the Transportation Research Board, No. 1928, Transportation Research Board
of the National Academies, Washington, D.C., pp. 118-125.